



# Taphonomic analysis on Neogene ostracods from Solimões formation, Borehole 1AS-5-AM, Brazil: A tool to the paleoenvironmental reconstitution

Katiane Silva dos Santos<sup>a,\*</sup>, Maria Inês Feijó Ramos<sup>b</sup>

<sup>a</sup> Graduate Program in Geology and Geochemistry, Instituto de Geociências, Universidade Federal Do Pará, Rua Augusto Correa S/n, Belém, PA, Brazil

<sup>b</sup> Museu Paraense Emílio Goeldi, Coordenação de Ciências da Terra e Ecologia, Av. Presidente Tancredo Neves 1901, Belém, PA, Brazil

## ARTICLE INFO

### Keywords:

Ostracods  
Fossil diagenesis  
Biostratigraphy  
Lacustrine environment  
Miocene

## ABSTRACT

The taphonomic analysis on the Neogene ostracods from the Solimões Formation (core 1AS-5-AM, Atalaia do Norte, Brazil) reflect conditions predominantly of early (film mineralization and mold formation) and late (recrystallization, iron oxidation and secondary gypsum) diagenesis. Fragmentation, disarticulation (from death, ecdysis, and transport of ostracods), bioerosion (by the action of chitinolytic bacteria) and transport were observed during the biostratigraphic process. Fossil-diagenetic analyzes through MEV, EDS, X-ray diffraction in sediments and ostracods valves and petrographic thin section, point to the non-replacement of the original chemical constitution of the most carapaces, but mineral filling with pyrite, dissolution, color change and recrystallization may occur. Based on these analyzes and on the lithological characteristics, the environment was interpreted as lacustrine, of low to moderate energy. The absence of evaporitic minerals and pyrite dispersed in the sediments attest to the low salinity of the environment. Three intervals were observed in the core according to the preservation patterns of the ostracods. In interval I (lake bottom), juvenile allochthonous ostracods suggest post-mortem transport. In interval II, the predominance of autochthonous fauna shows a low energy environment. Allochthonous and autochthonous (predominant) ostracods of interval III reflect energy variation in a scenario close to the coastal zone of lake.

## 1. Introduction

Among the Western Amazon Neogene invertebrates, ostracods stand out for their great abundance and diversity (Whatley et al., 1998; Muñoz-Torres et al., 2006). Taxonomic (Gross et al., 2013, 2014; Ramos, 2006; Whatley et al., 1998; Purper and Ornellas, 1991; Purper and Pinto, 1983), paleoenvironmental, biostratigraphic (Gross et al., 2013, 2014; Muñoz-Torres et al., 2006) and geochemicals studies (Gross et al., 2011, 2013, 2015) suggest that the ostracod assemblage of this region established itself in a predominantly lacustrine environment during the Miocene, although sporadic marine incursions have been suggested (Linhares et al., 2011, 2017, 2019; Leandro et al., 2022). Despite the great contribution of these studies, this is the first to present fossil-diagenetic implications of Miocene ostracods in this region to assist the paleoenvironmental interpretations.

Ostracods have a carapace ultrastructure mainly composed of fine crystals of primary low-magnesium calcite (Keyser and Walter, 2004) and trace elements such as magnesium, strontium, and stable-isotope as carbon, oxygen, and barium (DeDeckker, 2017). The carapace of

ostracods, since its formation, has the potential to preserve geochemical information, since these microcrustaceans incorporate these elements from the host water to synthesize their carapace (Turpen and Angell, 1971). However, during the fossilization process, these carapaces undergo chemical transformation as pyritization (Siveter et al., 2014), phosphating (Matzke-Karasz et al., 2013), calcite recrystallization (Bennett et al., 2011), silicification (Wilkinson et al., 2010), iron oxidation (Williams et al., 2008) and dolomitization (Bertanni and Carozzi, 1985).

In this article, the role of sedimentary diagenesis in the state of preservation of Miocene ostracods of the Solimões Basin, southwestern Amazon region is investigated. The results show the importance of these studies as a preliminary tool to geochemistry analysis and to the paleoenvironmental interpretation.

## 2. Materials and methods

The 55 sediment samples analyzed come from the core 1AS-5-AM (S 04° 29'/W 70° 17'), drilled near the village of Cachoeira, close to Itacuaí

\* Corresponding author.

E-mail addresses: [katisanti19@yahoo.com.br](mailto:katisanti19@yahoo.com.br) (K. Silva dos Santos), [mramos@museu-goeldi.br](mailto:mramos@museu-goeldi.br) (M.I. Feijó Ramos).

river, Amazonas state, Brazil, a region within the geological context of the Solimões Basin (Fig. 1).

The sedimentary samples were characterized by their granulometry, texture, color, and presence or absence of fossils. Part of the samples were treated by the usual methods for calcareous microfossils from which 180 g of dry sediment from each sample were soaked in a glass beaker with tap water, washed, and sieved in 32, 60, 80, and 115 mesh sieves. The residual material from each sieve was dried in an oven at 50 °C, for further screening of microfossils. The microstructure of the ostracod valves and carapaces from the core samples were performed using a TESCAN Scanning Electron Microscope and the chemical composition using energy dispersive spectrometry (EDS). Recent valves were also used for comparative analysis. For these analyses, specimens of fossil ostracods with valves and carapaces with different colors and preservation were selected. The specimens examined in this step were cleaned with deionized water and an ultrasound bath to remove the dirt and to identify the variations in composition along the structure of the valves (DeDecker, 2017).

This step was carried out at the Scanning Electron Microscopy Laboratory of the Museu Emílio Goeldi (MPEG), Belém, Brazil. In addition, the mineralogical characterization of the sedimentary matrix and ostracod valves were performed using X-ray diffraction (XRD) at the X-ray Diffraction Laboratory of the Geoscience Institute of the Federal University of Pará, in Belém, Brazil. Also, petrographic thin section of some samples was prepared in the petrography laboratory of the UFPA Geoscience Institute (Fig. 2).

To the populational structure analysis of the ostracods assemblage we followed Brouwers (1988) and Boomer et al. (2003) models and others references herein cited.

Subsequently, the analysis and quantification of valves and carapaces with distinction of color, size (ontogenetic stages) and preservation (fragments x valves and whole carapaces) were performed using a stereomicroscope. Data were organized and analyzed using graphics from the Mischke et al., 2014 program.

### 3. Geological settings

The Solimões Basin is a Paleozoic, intracratonic basin, with about 480,000 km<sup>2</sup> of total sedimentary area in the state of Amazonas, limited to the north by the Guianas Shield, to the south by the Brazilian Shield, to the east by the Arc from Purus and west by the Arch of Iquitos (Eiras et al., 1994; WanderleyFilho et al., 2010). The Solimões Formation comprises the Neogene portion of the basin and is characterized by greenish gray to dark gray claystone and siltstone interspersed with lignite. The fine to medium sandstone are greenish gray, sometimes yellow and brown. Breaches with carbonate concretions, gypsum, ferruginous, and lignite intercalations also occur. At the top of the section, the sandstone is white, poorly consolidated, fine to coarse. The sedimentation of these deposits took place in a fluvio-lacustrine environment, mainly based on outcrops samples (Maia et al., 1977; Caputo, 1984; Latrubesse et al., 2010; Gross et al., 2011; Nogueira et al., 2013). The thickness of the Solimões Formation can reach up to a thousand meters on the border between the states of Amazonas and Acre (Latrubesse et al., 2010). The deposits of this unit are covered discordantly by the Içá Formation (Maia et al., 1977; Nogueira et al., 2013) and have discordant inferior contact with the Alter do Chão Formation (Eiras et al., 1994).

Paleontological studies carried out in the Solimões Formation show a

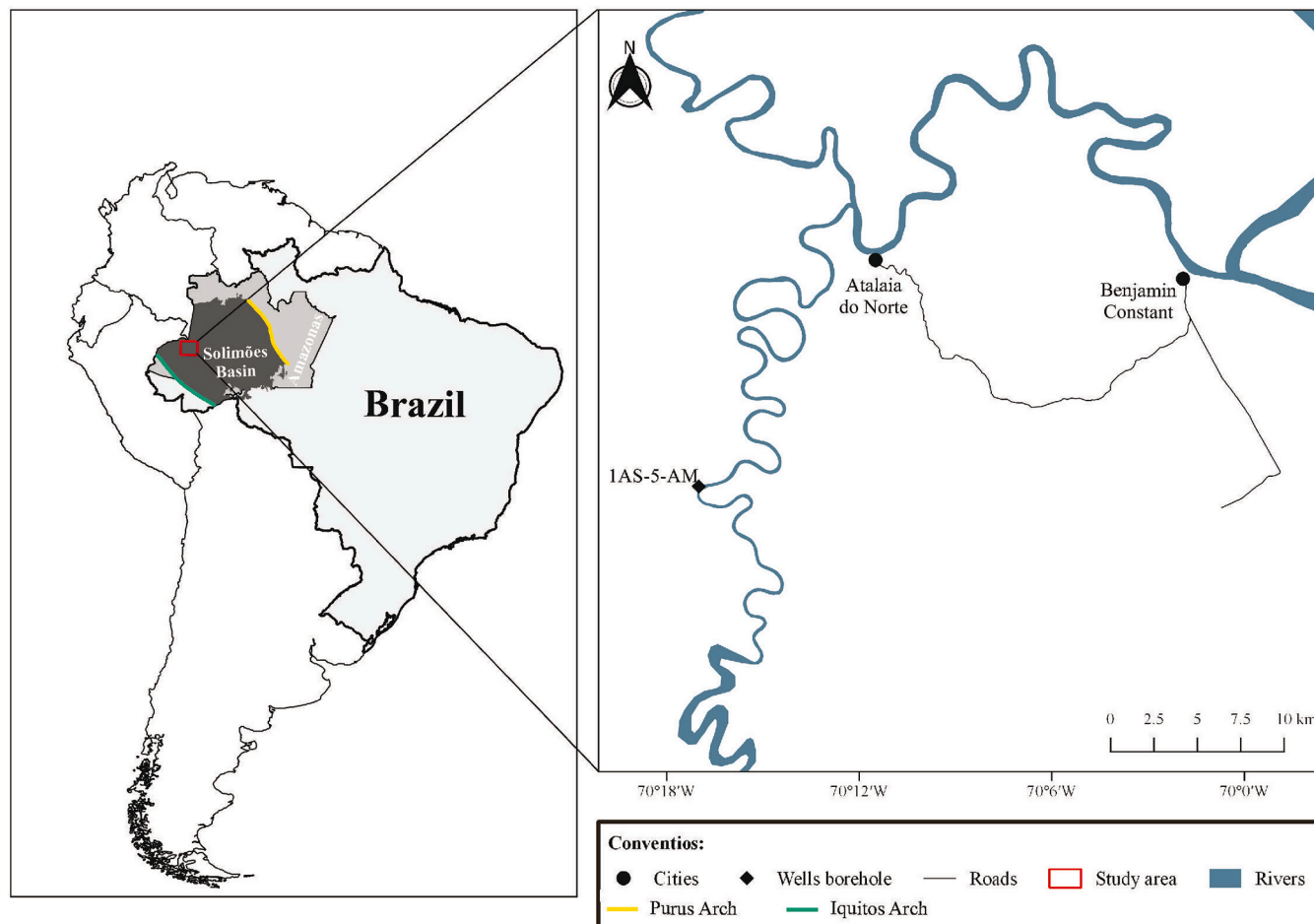


Fig. 1. Location of the study area. Source: author.

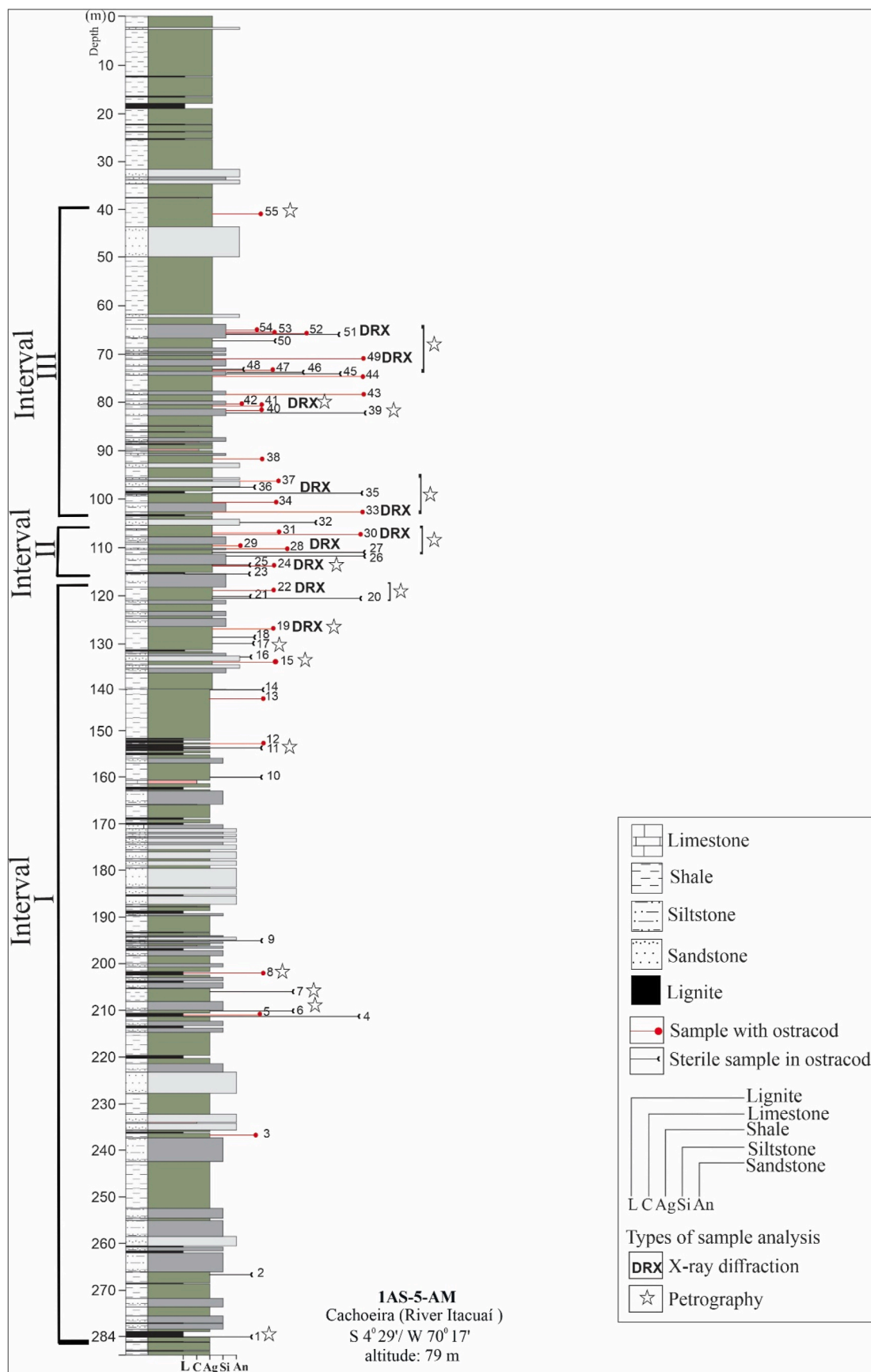


Fig. 2. Stratigraphic section of core IAS-5-AM with indicating of the ostracods samples and types of analysis. Source: author.

diversified fossiliferous content, consisting of ostracods (Gross et al., 2014; Linhares et al., 2017), mollusks (Wesselingh et al., 2002; Wesselingh and Ramos, 2010), foraminifera (Linhares et al., 2011), fish, birds, reptiles (Latrubesse et al., 2010) and wood (Machado et al., 2012), which were established within a complex fluvio-lacustrine paleoenvironment, with swamps and deltas associated. This large system is recognized as “Lake Pebas” (Wesselingh et al., 2002) and/or “mega-wetland” (Hoorn et al., 2010). It is also worth mentioning the hypothesis of marine incursions in the paleoenvironments of the Solimões Formation, which were evidenced mainly based on the micropaleontological content (Hoorn, 1993; Jaramillo et al., 2017; Linhares et al., 2011, 2017, 2019; Leandro et al., 2022). Evidence of marine influence in the sedimentary record is still scarce, except for the records by Räsänen et al. (1995) and Nogueira et al. (2003).

The stratigraphic range of the Solimões Formation was inferred from biostratigraphic studies with palynomorphs, mollusks and ostracods (Cruz, 1984; Hoorn, 1994; Wesselingh et al., 2002; Silveira and Souza, 2017; Muñoz-Torres et al., 2006; Linhares et al., 2019) which allowed to propose biozones ranging from the early Miocene to the Pliocene.

#### 4. Results and discussions

The recovered ostracod assemblage corresponds to 998 carapaces, 2,598 valves, 3,193 fragments and 214 carapace molds (Fig. 3). In addition, during the screening stage, gastropods, bivalves, charophytes, foraminifera, decapod fragments (Fig. 5B), teeth, vertebrae and fish scales were recovered.

Among the ostracods, 99% belong to the genus *Cyprideis*, however other genera and species, such as *Skopaeocythere tetrakanthos* (eleven valves and one juvenile carapace), *Perissocytheridea* (six valves) and *Pellucistoma* (four valves) were also registered; this assemblage is restricted to sample 28, which presents an expressive abundance of well-preserved ostracods and with different ontogenetic stages, as well as a significant number of foraminifera of the genus *Ammonia*.

##### 4.1. Quantitative and qualitative analysis of the ostracod assemblage

Quantitative and qualitative analysis of the ostracod assemblage as well as the lithological characteristics allowed the individualization of three intervals for the analyzed core (Fig. 4).

Interval I (284.50–119.30 m): from the most basal portion of the core, 22 samples were selected, of which 13 are barren for ostracods.

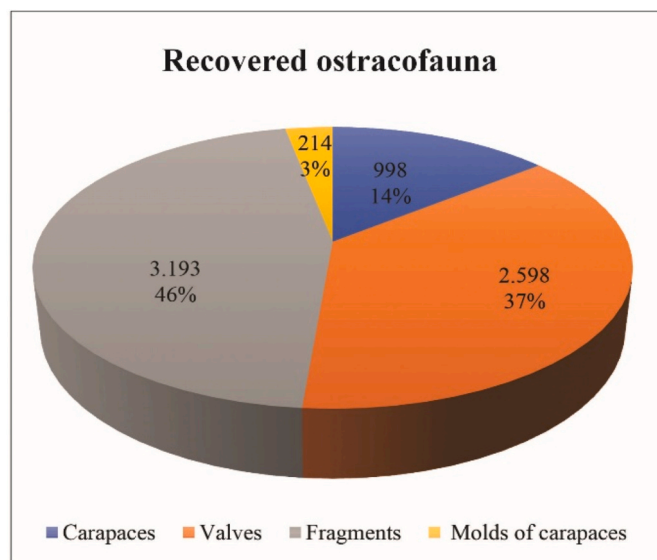


Fig. 3. Quantitative relationship of recovered ostracod assemblage. Source: author.

The gray claystone (Fig. 5G) is locally lignite, while siltstone is greenish gray (Fig. 5F); there are also massive black claystone, rich in organic matter and lignite fragments (Fig. 5 E). The massive structure is predominant in the samples, with small laminations being observed in sample 1. The most friable claystone corresponds to the samples with the greatest amount of lignite fragments. In samples with higher organic matter content, ostracods are rare, as are other bioclasts; when recovered, they are poorly preserved. Compared to the other intervals, this is the one with the smallest number of ostracods, of which only 62 specimens correspond to entire valves and carapaces, while 67 are fragments, 47 are equivalent to internal molds of pyritized carapaces and 4 valves show partial dissolution. Most of the pyritized ostracod molds are concentrated in solid black clay and correspond only to closed carapaces. In medium gray clays, the organic matter content is still visibly significant. Only 11 molds were recovered from this lithology. White and slightly gray to white valves and carapaces with a milky (whitish) appearance are common in light greenish gray claystone, except for sample 19, which showed colors reddish brown, dark gray and some completely black valves.

Interval II (116.70–107.10 m): between the depths 116.70 m–107.10 m, 9 samples were selected, of which 4 are barren for ostracods. The lithology corresponds only to massive claystone, and locally light gray green siltstone (Fig. 5D). The packing degree of the bioclasts is of the loosely packed to dispersed type. The content of organic matter and lignite fragments in the sediment are much lower than the other intervals (I and III), given by the lighter tone presented by the samples. This interval stands out for presenting the greatest abundance of ostracods as well as other bioclasts, with an excellent state of preservation. The recovered ostracod fauna corresponds to 2595 whole ostracods, 2424 fragments, 103 with signs of partial dissolution and only 4 molds of pyritized carapaces. Ostracods recovered from this range exhibit light to dark gray, amber, milky white, hyaline, and golden colors; the latter is more frequently seen in the internal view of the valves. Only in sample 29 all ostracods show reddish brown color.

Interval III (106.90–41.00 m): this range comprises 24 samples, 10 of which are barren for ostracods. The lithology is characterized by massive, greenish gray claystone, locally siltstone, with *Skolites*-type bioturbations (Fig. 5 A and C). The organic matter content is relatively lower than in samples from interval I. Once again, lignite fragments give a friable appearance as their content increases in the samples.

This interval has the second largest number of ostracods when compared to the others, but their preservation status is lower than those presented in interval II (116.70 m–107.10 m).

The retrieved ostracod assemblage is equivalent to 1011 whole ostracods, 530 fragments, 204 with signs of partial dissolution and 162 molds of pyritized carapaces, constituting the interval with the highest concentration of molds. The valves and carapaces are, in order of abundance, light to dark reddish brown, light to dark gray, amber and white with a milky appearance.

##### 4.2. Biostratigraphic analysis

###### 4.2.1. Transport and energy from the depositional environment

The analysis of the population structure through the adult:juvenile ratio, as well as the valve:carapace, allowed us to verify the degree of transport suffered by the ostracod assemblage. The results obtained reveal allochthonous and autochthonous associations in the three identified intervals. The A/J ratios ranging from 2/1 to 6/1 (Chart. 1) reveal the predominance of adults, which according to the Brouwers (1988) model, reflects high-energy environmental conditions. However, the data obtained in the present study suggest that probably the elimination of part of the juveniles may have occurred by mechanical breakage of slightly calcified valves during the removal of the sedimentary matrix and by dissolution, thus implying a greater number of adults.

Following the proposal by Boomer et al. (2003) associations with

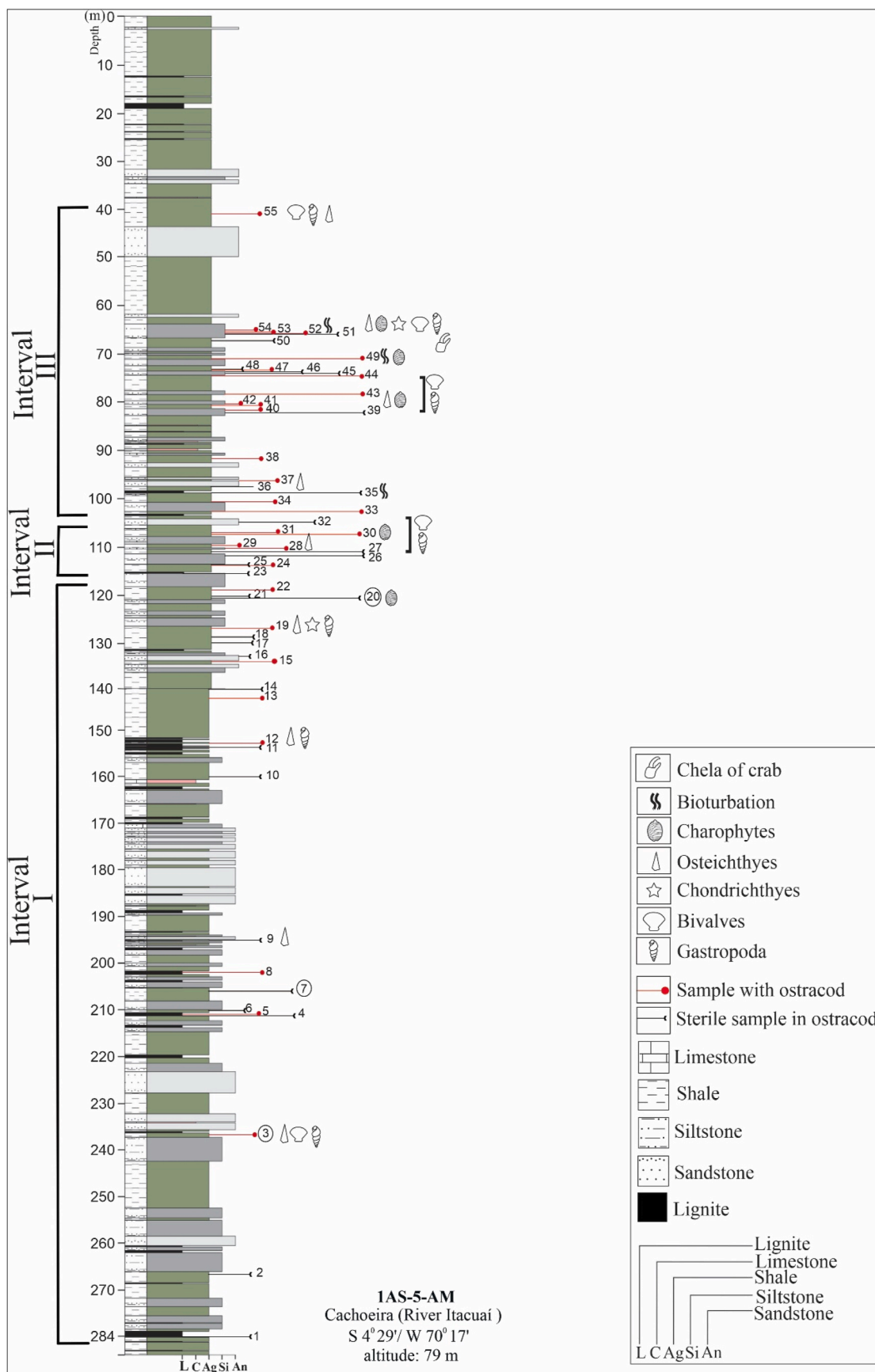


Fig. 4. Lithological profile of core 1AS-5-AM with the distribution of microfossils and individualization of intervals. Source: author.



**Fig. 5.** Interval III- A) sample 52 (massive, greenish gray claystone, locally siltstone, with Skolites-type bioturbations), B) sample 50 (massive, greenish gray mudstone with chelas of decapod-white arrows), C) sample 35 (massive, greenish gray mudstone, with Skolites-type bioturbations-red arrows). D: interval II- D) sample 28 (light gray green claystone, rich in ostracods, gastropods, bivalves, foraminifera). E-G: interval I- E) sample 7 (massive black claystone), F) sample 20 (massive, greenish gray claystone), G) sample 3 (massive gray claystone). Source: Author.

predominance of adults and/or a mixture of adults and juveniles indicate a thanatocenosis. In the analyzed samples, it was possible to identify low and high energy thanatocenosis, the first being more common in interval II and the second in interval III (Chart. 1). Sample 28, for example, has a higher number of adults than juveniles, but the latter are provided with juvenile stages A-1 onwards, featuring a low-energy thanatocenosis, which reflects minimal displacement conditions.

In contrast, representative samples of high-energy thanatocenosis, such as 53, juveniles only correspond to stages lower than A-1, with a predominance of adults, which indicates relative post-mortem agitation by currents and/or bioturbation organisms.

Interrupted thanatocenosis configurations that mostly present juvenile carapaces (Boomer et al., 2003). These were identified only in samples 24 (interval II), and in samples 33 and 49, both from III. The A/J ratios found respectively correspond to 1/31, 1/8 and 1/27.5, which suggest fauna deposited in a calm environment, as evidenced by the predominance of juvenile specimens (Brouwers, 1988). This large number of juvenile ostracods also suggests high juvenile mortality (Whately, 1988), probably caused by environmental stress conditions such as changes in temperature, dissolved oxygen levels, salinity or may be related to rapid burial events (DeDeckker, 2002). This last hypothesis is evidenced in sample 49 by the amount of pyritized ostracod molds,

since the genesis of the molds required fast burial conditions.

Sample 49 has a significant amount and a high proportion of juvenile carapaces and valves, characteristics that could lead to the interpretation of both a taphocenosis and an interrupted thanatocenosis. As the most likely scenario, it is suggested that some rapid burial event (Whatley, 1988; Holmes, 1992), promoted by influxes of river terrigenous, has buried juvenile ostracods still alive, along with the discarded valves from the ecdysis, once the ostracods juveniles disarticulate their carapaces after ecdysis (Whatley, 1988; Holmes, 1997). Death by asphyxia due to rapid burial is suggested for the high preservation of juvenile articulated carapaces, which configures an interrupted thanatocenosis. Holmes (1992) points out that many carapaces can indicate a very fast sedimentation rate or reflect low energy conditions.

Taphocenosis configures an allochthonous association and in the identified intervals, they represent A/J ratios ranging from 1/4 to 1/9.5 in the I. In interval II it is equivalent to 1/12.9; while in III, it ranges from 1/1.4 to 1/9.8 (Table 1). These reasons reveal the predominance of juvenile ostracods. Brouwers (1988) infers that the predominance of juvenile specimens indicates fauna deposited in a calm environment; Boomer et al. (2003) infers that a taphocenosis is indicative of *post-mortem* transport of juvenile specimens from a higher energy environment to a lower energy environment. Some of the allochthonous fauna specimens from interval II (sample 30) correspond to delicate, hyaline and well-preserved valves, which suggest a short transport distance.

Ideal preservation conditions with a population structure close to a real association was observed only in sample 33 through the A/J ratio of 1/8 (interval II), where for each adult, there are eight juveniles.

The population structures found show that the energy conditions in interval III oscillated from high to low, which resulted in associations of allochthonous (taphocenosis) and autochthonous (thanatocenosis) ostracods, respectively. It is suggested as a scenario for energy variation the shallower parts of a lake, close to the lake's coastal zone, where the influence of winds on its surface is greater, generating different hydraulic gradients (Namiotko et al., 2015).

In interval II, the predominance of thanatocenosis shows a low energy environment, the result of which is corroborated by the abundance and excellent state of preservation of the ostracod assemblage, reflecting little hydraulic reworking (Namiotko et al., 2015).

In interval I, allochthonous ostracods suggest transport (except sample 3) under conditions of higher energy, inferred by the incidence of disarticulated juvenile valves.

Probably, the disarticulation of juvenile carapaces occurred through transport, which were transported from the shallower parts and with the cessation of energy, were deposited in the deep part of the lake, where deposits of disarticulated juvenile valves are common (Danielopol et al., 2002; Zhai et al., 2015). The lake bottom is corroborated by the sedimentological characteristics and low degree of preservation of the valves

due to inappropriate habitat conditions (anoxia, acidic pH).

#### 4.2.2. Fragmentation

Fragmentation was more evident in the intervals with the greatest number of recovered ostracods. However, interval I is the most affected, where fragments correspond to 52% (Fig. 6) of the total number of specimens.

In interval II (116.70–107.10 m) the sample 28 (110.20 m) presents the most abundant ostracod assemblage, with a high number of whole ostracods, which were preserved in situ. However, 49% (2164) of the assemblage in this sample corresponds to fragments of very thin valves (little calcified), which mostly have sharp edges (Fig. 7B) in addition to many bivalves and gastropods. The suggested hypothesis is that the action of winds on the surface of the water body, where these organisms lived, may have generated small currents at the bottom of the substrate. Ostracods with thinner carapaces may have been suspended, which caused the collision with larger bioclasts (bivalves and gastropods), resulting in valve breakage. For Kihn et al. (2017) more fragile (thin) and poorly ornamented valves are more susceptible to fragmentation. Another condition suggested for fragmentation of interval II may also be related to the stage of recovery of the ostracods from the sedimentary matrix (during sieving). According to DeDeckker (2002), ostracods tend to fragment under light pressure conditions due to thin carapace thickness. Interval III has the lowest percentage of fragments, and the suggested causes are the same as for Interval II.

In the analyzed samples, influence of chemical origin (dissolution) in the fragmentation is suggested for the samples of interval I and III, due to the occurrence of poorly preserved fragments and with pore-channels expanded by dissolution. The increase in the pore-channels of the valves may have generated a network of holes, making the valves more susceptible to breakage as dissolution progresses in these places (Danielopol et al., 1986).

For interval II, the dissolution hypothesis is discarded due to the low number of fragments by dissolution and the good preservation of the specimens. The influence of biological origin for fragmentation is also unlikely, since only eight valves with bioerosion were observed in interval II alone.

#### 4.2.3. Bioerosion

During SEM analysis, the presence of bioerosion was observed in eight valves as in sample 28 (Fig. 7A). This biodegradation is characterized as trails left by chitinolytic bacteria after consumption of the chitinous coating, which covers the carapace of the ostracods. In environments with low sedimentation rates, many valves can present this type of biodegradation, as chitinolytic bacteria are aerobic and prefer oxygenated environments at the water-sediment interface. Thus, with increasing depth, the action of chitinobacteria decreases (Danielopol

**Table 1**

Elements and their percentages of occurrence in valves of different colors identified by EDS analysis. Source: Author.

Elements	Dark gray valve		White valve		Amber valve		Brown valve Reddish	
	28	30	28	49	28	49	28	49
Spectra	1	2	1	3	1	2	1	3
Carbon (C)	23.82	27.18	14.85	15.95	15.80	24.34	0.00	18.26
Oxygen (O)	52.05	52.52	52.58	55.48	52.98	55.18	45.86	59.12
Calcium (Ca)	11.80	18.73	32.26	28.56	29.38	20.01	10.31	21.25
Sodium (Na)	0.34	0.15	0.00	0.00	0.00	0.00	0.00	0.00
Magnesium (Mg)	0.00	0.26	0.31	0.00	0.11	0.00	0.00	0.23
Manganese (Mn)	0.00	0.19	0.00	0.00	0.00	0.00	2.37	0.26
Aluminum (Al)	0.39	0.16	0.00	0.00	0.00	0.00	0.00	0.00
Iron (Fe)	0.00	0.26	0.00	0.00	1.58	0.48	38.58	0.88
Phosphorus (P)	0.00	0.00	0.00	0.00	0.00	0.00	0.53	0.00
Sulfur (S)	11.03	0.15	0.00	0.00	0.00	0.00	0.22	0.00
Silicon (Si)	0.44	0.40	0.00	0.00	0.15	0.00	1.68	0.00
Potassium (K)	0.12	0.00	0.00	0.00	0.00	0.00	0.33	0.00
Chlorine (Cl)	0.00	0.00	0.00	0.00	0.00	0.00	0.13	0.00

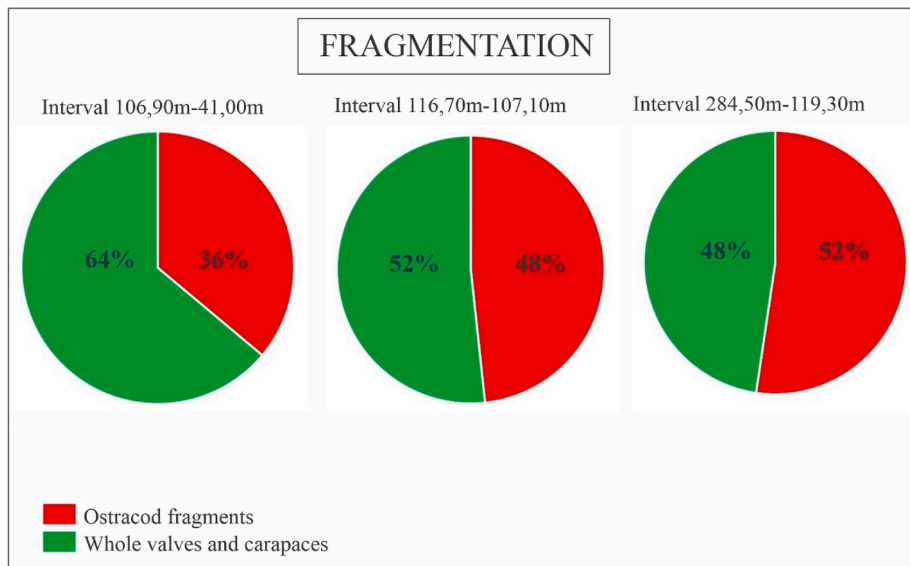


Fig. 6. Percentage graph of fragmentation per interval. Source: Author.

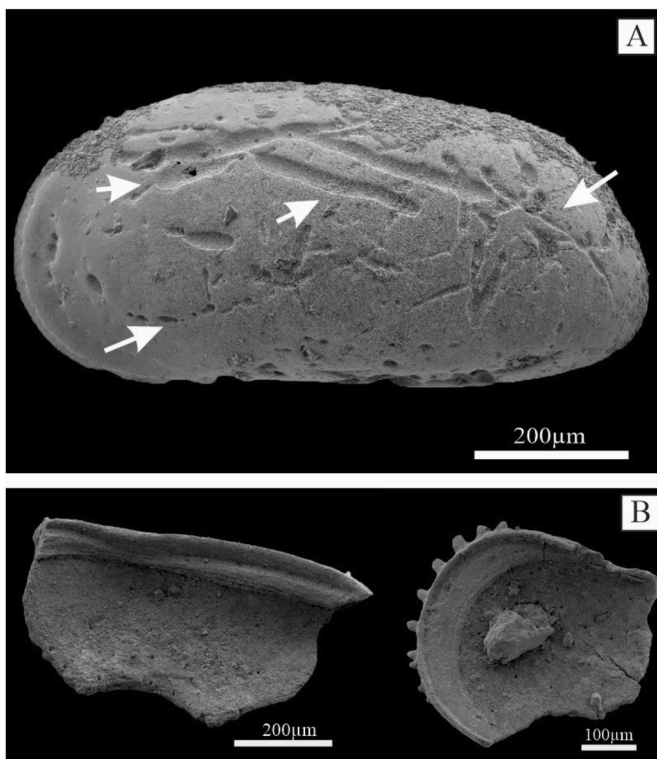


Fig. 7. A–B: SEM images. A) Sample 28 (bioerosion observed in valves, indicated by white arrows). B) Common shapes of valve fragments. Source: Author.

et al., 1986; Namiotko et al., 2015). The occasional occurrence of bioerosion could even be indicative of a high sedimentation rate for the study area, but the high amount of valves/carapaces covered by mineral films may have obliterated the visualization of this taphonomic damage, since bioerosion was only observed in hyaline valves.

#### 4.2.4. Disarticulation

Disarticulation was one of the taphonomic signatures that most affected the ostracods in the study area. The data obtained suggest that disarticulation was mainly favored by death, followed by ecdysis and, to

a lesser degree, by transport.

In the comparison between the three intervals, there was a greater occurrence of disarticulated valves in interval II, which presents a predominance of adult valves and a significant number of juvenile valves (Fig. 8). In contrast, in III the juvenile ostracod valves predominate. In general, the number of disarticulated valves is greater than the number of articulated carapaces in the three intervals, except for samples 24 and 33. Samples with less than two valves/carapaces were not considered.

As a cause for the disarticulation of interval I, transport to the disarticulated valves of juveniles in samples 19 and 13 is suggested, as evidenced in the analysis of the population structure. For the disarticulated adult valves in sample 3, it is inferred that they are due to natural death (Whatley, 1983), since there is evidence that the ostracods, at this depth, was preserved in situ.

Disarticulation may also be due to the molting process (Danielopol et al., 1986; Whatley, 1988; Do Carmo et al., 1999) as well as after death (Whatley, 1983). The predominance of adult valves in interval II may indicate that disarticulation is due to death and not ecdysis, since the molting process ceases in ostracods after reaching the adult stage (Smith and Horne, 2002). Except for sample 30, the in-situ preservation evidenced in this interval excludes transport as an agent of carapace disarticulation.

The predominance of juvenile valves in interval III may suggest that the underdeveloped hinge and transport, both favored by the small size of the specimens (Zhai et al., 2015; Park et al., 2003), were the main factors that favored the disarticulation of the ostracods in this interval.

### 4.3. Fossil diagenesis

#### 4.3.1. Chemical and mineralogical characterization of ostracod valves and sediments

An integrated analysis of EDS and XRD in ostracods valves and sediments was made allowing the follow results. The EDS analyzes in well-preserved, white-colored fossil ostracod valves present in the core analyzed here, show that the original chemical composition was maintained (Fig. 9A). It could be confirmed through the comparative analysis of Recent ostracod valves that were also tested (Fig. 9B).

Recrystallization was observed only in some valves in samples 49 and 19. Recrystallized valves have a granular texture and crystals with euhedral faces 2.5–4 µm in diameter. Both recrystallization textures are like those described by DeDecker (2002) and Bennett et al. (2011). EDS analysis of recrystallized valves confirms that the original chemical

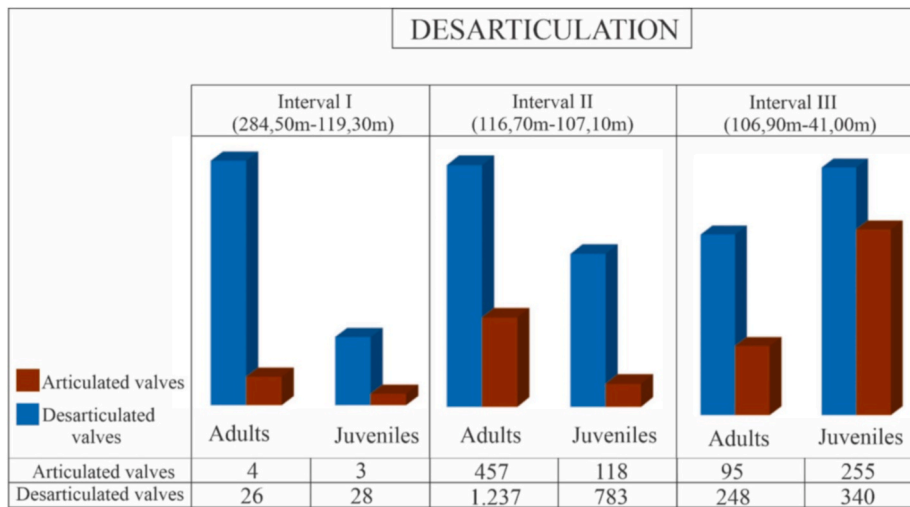


**Fig. 8.** Percentage bar graph number of articulated versus disarticulated ostracods valves per interval. Source: Author.

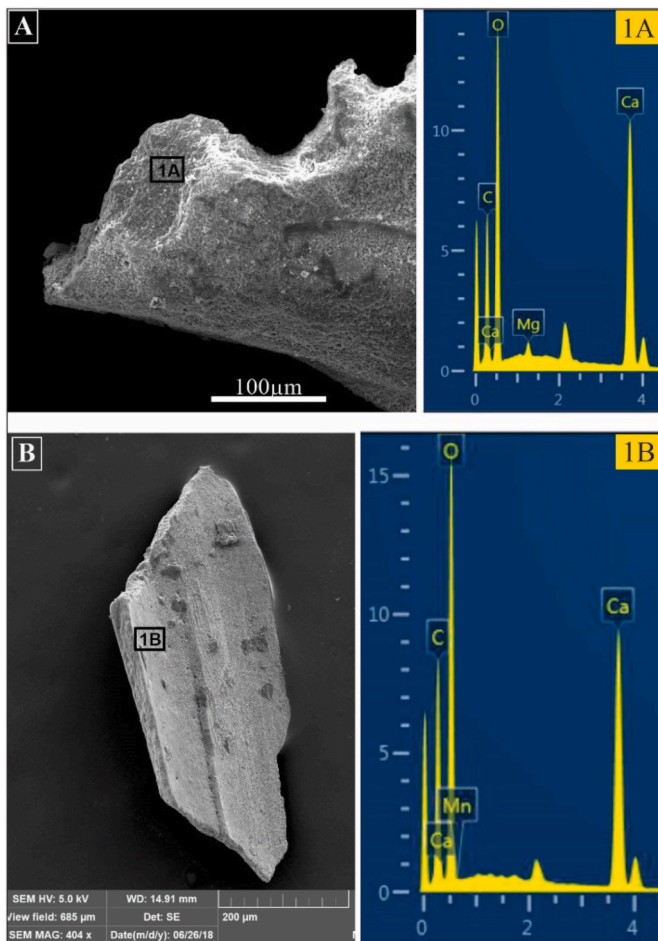


**Fig. 9.** SEM images and spectrum generated from EDS. A) Fossil ostracod valve. B) Recent ostracod valve. 1 A) Chemical composition of well-preserved white fossil valve from the present study. 1 B) Chemical composition of Recent valve. Source: Author.

composition was maintained.

Different colors were also observed in some ostracod's valves during the fossil-diagenetic process (Fig. 10). In Table 1, the EDS analysis in the valves discriminates which chemical elements provided by sample

sediments contaminated the valves changing the color of them. Table 2 shows the results of XRD analysis in the sediment samples and some minerals that participated in the fossil-diagenetic processes of color change mineralization (pyrite formation).

In the reddish-brown valves (Fig. 11A), in spectrum 1, Fe, P and O peaks show the presence of iron phosphate (Table 1); it is related to the abundant mineral giniite present in the sedimentary matrix of this sample (Fig. 11B). Still in spectrum 1, Si, K, Ca, and Mn peaks suggest the contribution of siliciclastic sediments and clay minerals. The S peak may indicate the sulphide mineral phase. The low concentration of Cl peak suggests an association with sediments. Spectrum 2, coming from the valve surface without a mineral film, evidenced the presence of calcite (Ca, O, C) as well as Fe and Mn peaks, which indicate that they come from the mineral film that covered the valve. Spectrum 3 has the same composition as 2, however only the Mg peak was detected. Its occurrence only in the internal part of the lamella, free of adhering particles and its low intensity peak, suggests that the Mg corresponds to the original chemical composition of the carapace of the ostracods.

The spectrum generated on the surface of the amber colored valves (Fig. 12A) shows calcite (Ca, O, C), in addition to Fe, Si, Mg and Au - the last coming from the metallization process of specimens for SEM and EDS analysis; while in the inner portion of the lamella, only calcite and Fe were detected (spectrum 2) (Fig. 12B). Iron is the most common element and was detected in all amber-colored valves analyzed, which may indicate that this element, in its oxidized form, is responsible for this color change, also resulting in the contamination of specimens, as Fe is not part of the original chemical composition of the ostracods carapaces.

The gray colored carapaces/valves (Fig. 13A) are usually covered by thick black films. On the surface of these films, relatively high peaks of C (Table 1) and more discrete peaks of K, Si, Al, and Na were identified. Gypsum crystals (Ca, S, O peaks) cover the black film and portions of the valve (spectrum 1 and 3, Fig. 13B). Spectrum 2, the portion of the ostracod's valve not covered by the film, reveals Ca, O, C peaks and traces of S and Fe, which suggest iron sulphide (or monosulphide) mineral phase; Mg, Al, Na, Mn, and Si indicate a thin sediment contamination on the valve surface. Subsequently, the iron sulphide (or monosulphide) that covers the valve, when oxidizing, conditioned the formation of gypsum crystals, which covered the valve and the black film. Despite the formation of minerals on the surface of the valves, this process did not imply the replacement or loss of significant skeletal material from the calcite lamella in any of the specimens analyzed.

The carapace of the ostracods is composed of low magnesian calcite and in the analyzed valves, it was observed that the magnesium ranged

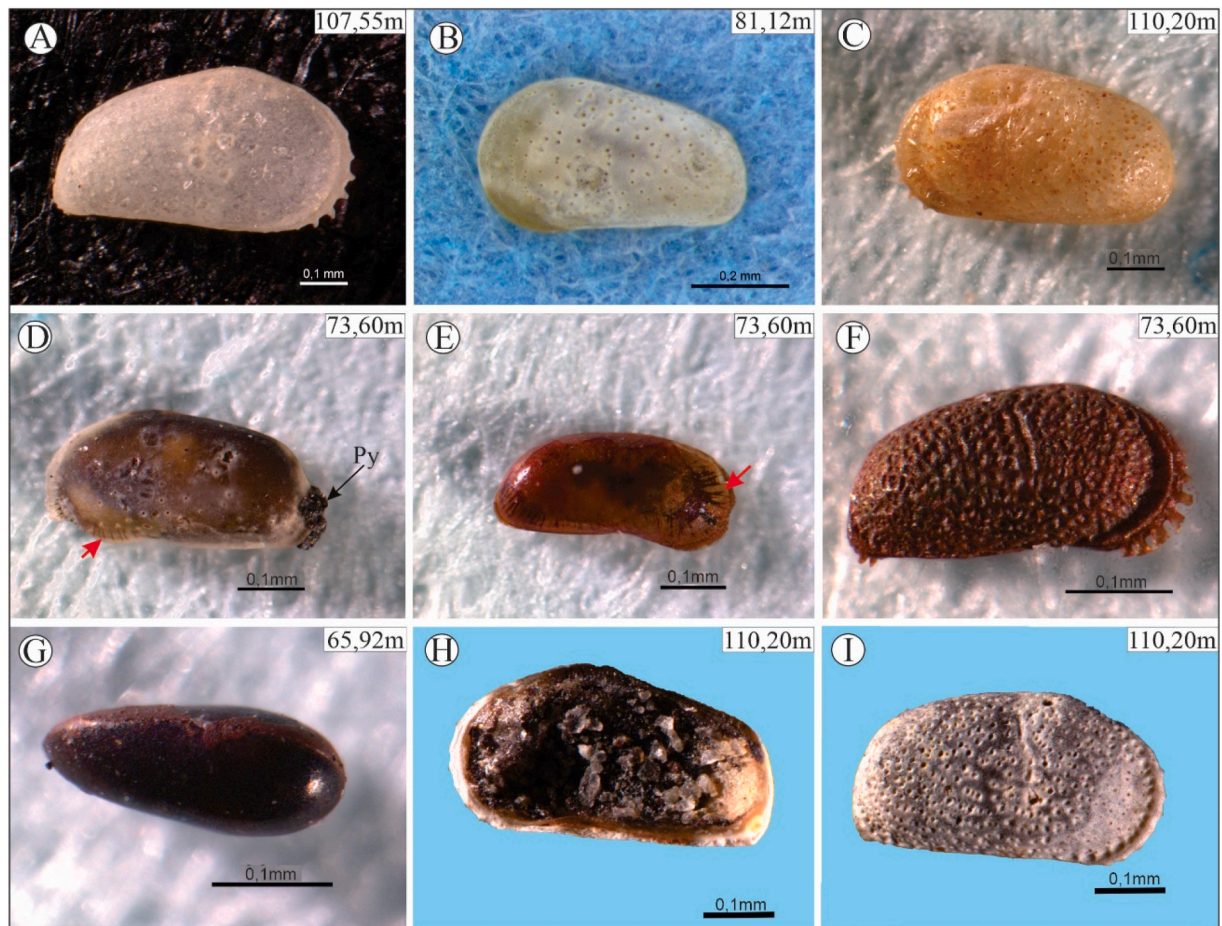


**Fig. 10.** Color variation of the ostracodes of the core 1AS-5-AM, images obtained by electronic magnifying glass. (A) Hyaline valve, without color change, well preserved. (B) Opaque white valve with a whitish appearance affected by partial dissolution. (C) Amber valve with very fine crystals of secondary gypsum, almost imperceptible, located in the center-upper portion in the anterior region. (D, E, F) Brown valve reddish covered with iron phosphate. Red arrows highlight the marginal pore-channels filled with iron phosphate, black arrow indicates the occurrence of overpyrite (D). (G) Black carapace, covered by iron monosulphide, with oxidized portions (reddish portions). (H–I) Gray valve. (H) Internal view partially covered by a thick black film, which is composed of siliciclastic sediments and iron monosulphide. (I) External view of the valve light gray.

**Table 2**

Minerals identified by XRD analyzes. Source: Author.

Sample	Identified minerals by XRD analyzes
Sample 19	Quartz, giniite, mica, kaolinite
Sample 22	Quartz, illite, kaolinite
Sample 24	Quartz, mica
Sample 28	Quartz, giniite, illite, birnessite, mica, hydroxalcite
Sample 29	Quartz, giniite, birnessite, mica, hydroxalcite
Sample 30	Quartz, hydroxalcite, montmorillonite, vermiculite
Sample 33	Quartz, giniite, birnessite, carlinita, mica
Sample 39	Quartz, giniite, mica
Sample 41	Quartz, birnessite, mica, montmorillonite
Sample 42	Quartz, giniite, birnessite, mica, hydroxalcite, vermiculite
Sample 49	Quartz, giniite, birnessite, mica, hydroxalcite

from 0 to a maximum of 0.55% in the well-preserved and uncolored valves. In the best-preserved valves, Mg peaks are very low, sometimes not even detected. In poorly preserved and/or color altered valves, magnesium is slightly higher, but does not exceed 0.90% of the total composition, suggesting the influence of the interaction of adhering minerals on the surface of the valves.

In general, in the analyzed specimens of ostracods, two samples had their valves affected by recrystallization; color-altered ostracods, despite preserving their original chemical composition, are contaminated by elements from clay minerals, pyrite films, iron mono-sulfate, iron oxide

and iron phosphate, and thallium sulphide adhered to the surface of valves/carapaces. These contaminating elements were detected within the calcite lamellae and not only on the surface of the valves. White valves exhibit their original chemical composition without any contaminating element; this result is expected, as usually color-altered valves present trace elements that are uncommon to their original chemical composition.

For Tucker (1990), low-magnesium calcite (or calcite with low magnesium content) is susceptible to the incorporation of smaller chemical and traces elements to its composition, as it is more stable against diagenetic changes. During diagenesis, through the percolation fluids, strontium, magnesium in smaller amounts, in addition to manganese and iron in more expressive amounts correspond to the elements that can be incorporated into the composition of low-magnesium calcite. In contrast, aragonite, and calcite with high magnesium content, as they are less stable, are more susceptible to substitution by calcite with high magnesium content (Bennett et al., 2011; Holmes and De Deckker, 2012). Thus, the constancy of Fe and Mg, in valves with color change and/or poorly preserved, observed in the present study, corroborate these elements as the main contaminants incorporated in the analyzed valves. The preservation of the original composition of the specimens also evidences the mineral stability of the carapace.

#### 4.3.2. Early diagenesis mineralization: pyrite formation

Pyrite occurs in three ways: as carapace molds (Fig. 14 A and B),

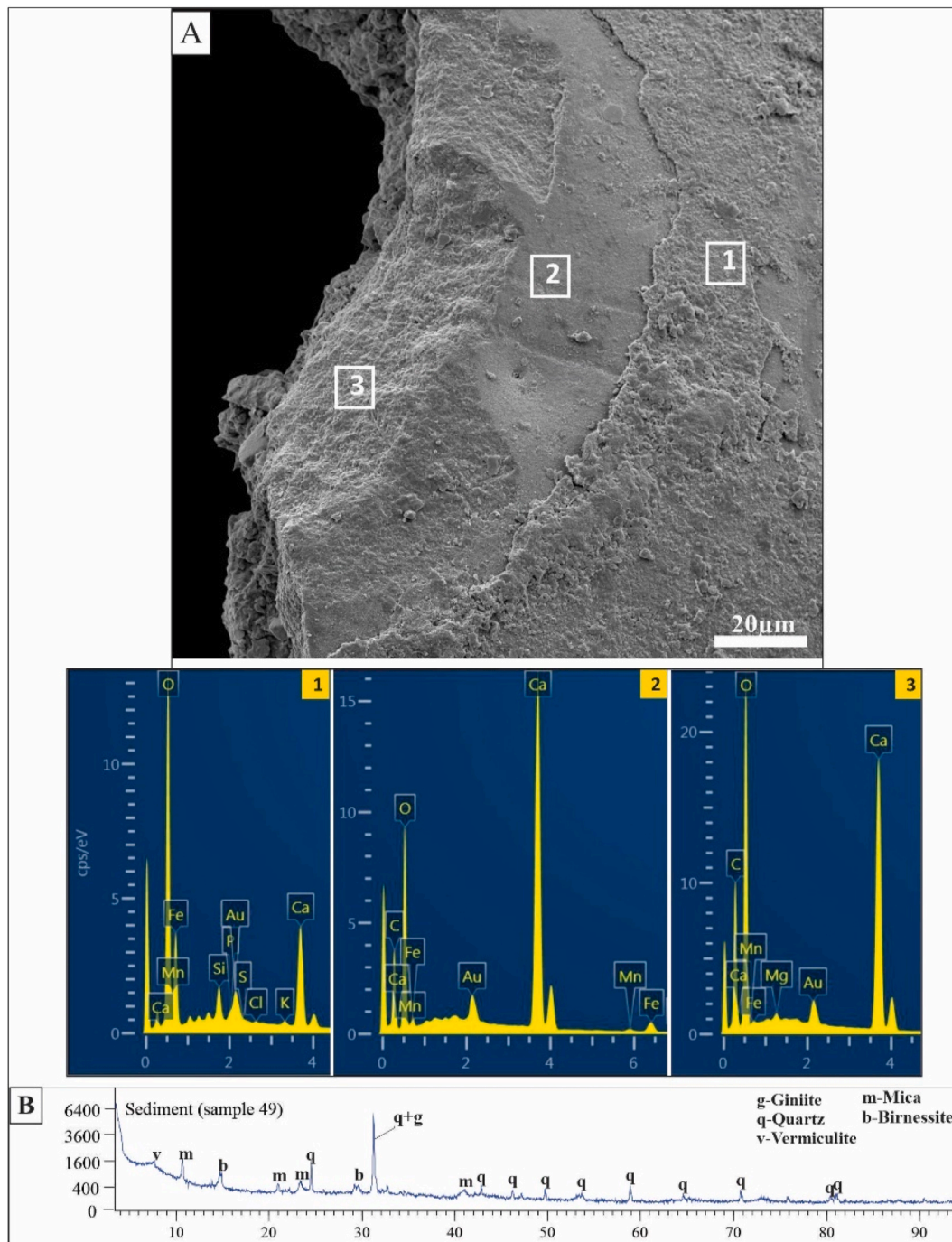


**Fig. 11.** (A) SEM photomicrography and EDS specters (1, 2, 3) in reddish-brown valve. (B) Diffractogram with the mineralogical composition of the sediments from where the valve came from. Source: Author.

encrusting on the surface of valves and carapaces (Fig. 15B), and filling the interior of carapaces (Fig. 15A and B). Such forms of occurrence are common in the three intervals, the most prominent being the presence of molds, whose formation occurred preferentially in samples where sediments contained the mineral Giniite (iron phosphate), except for sample 8.

A total of 214 molds were recovered and their distribution along the core is arranged as follows: in interval I there are 48 molds, in II, only 4, while in III, the highest occurrence of molds was recorded, corresponding to a total of 162 specimens.

Over-pyrite (Allison, 1990; Raiswell, 1997) corresponds to pyrite encrusting in pore-channels of the valves and in carapaces (Fig. 15 B),

being more common in intervals II and III. Pyrite filling of carapaces was observed in two specimens from samples 49 and 28, also affecting four valves from sample 31. Both styles of pyritization occurred punctually and always associated with molds.

When analyzing the molds via SEM/EDS, it was found that the pyrite had the framboidal habit, as well as euhedral crystals. Framboidal pyrite aggregates (Fig. 14A) are restricted to the molds of sample 8 only, while euhedral crystals (Fig. 14B) are common in the pyritized molds of the other intervals.

The presence of crust of yellow material covering all molds of sample 8 was also observed. EDS analysis in these specimens confirms the presence of natrojarosite by sodium (Na), sulfur (S) and iron (Fe) peaks

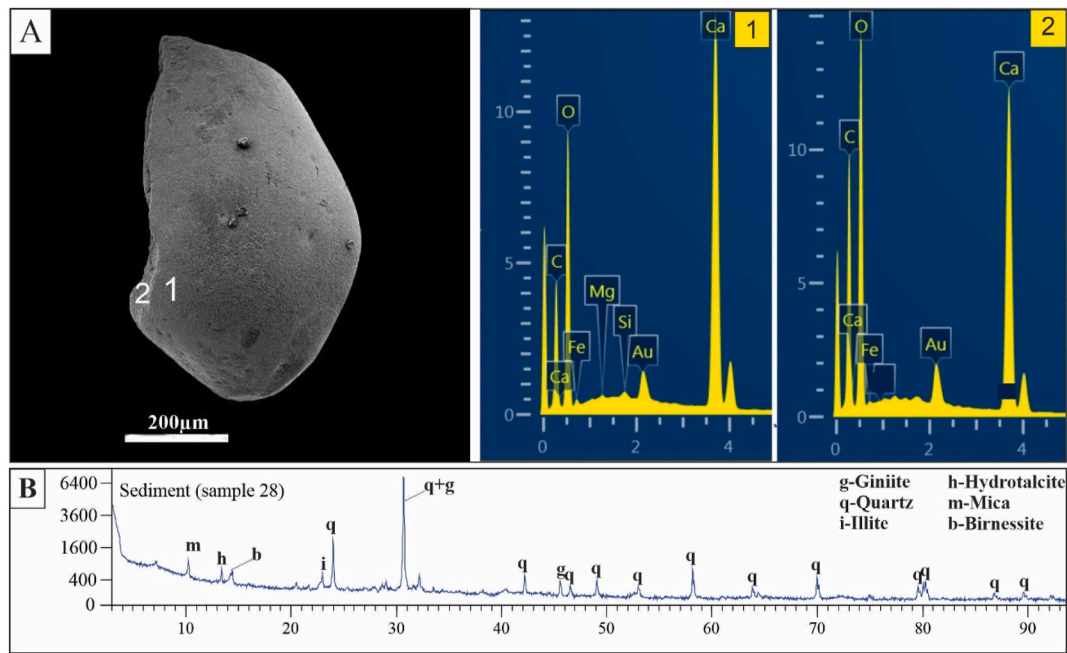


Fig. 12. (A) SEM photomicrography and the EDS specters (1, 2) in amber color valves. (B) Diffractogram with the mineralogical composition of the sediments from where the valve came from. Source: Author.

(Fig. 14B). Natrojarosite corresponds to a secondary sulfate, formed from the oxidation of pyrite when exposed to moisture (Urbani et al., 2016). The occurrence of this mineral suggests that the samples were probably exposed (sub-aerial exposure).

The presence of pyrite in the samples occurred only in the cavity and surface of the carapaces from the creation of a sulfuric microenvironment inside and around the carapaces (Palacios-Fest et al., 1994; Wang et al., 2013). Its widespread occurrence in sediments is absent, as corroborated by XRD analyzes in sediments (Table 2).

For the formation of pyrite associated with the carapaces of ostracods, it is suggested that a rapid burial event buried these microcrustaceans alive, leading to their death. After death, the decomposition of the soft parts by sulfate-reducing bacteria locally saturates the area around the carapaces in hydrogen sulphide. The latter reacted with the mineral giniite (iron phosphate), identified by XRD (Table 2), in the sediment matrix around the carapaces (Fig. 14A), which led to the mineralization of pyrite crystals.

The occurrence of internal molds and mineral filling only of closed carapaces indicate rapid burial, since the soft tissues decompose quickly (DeDeckker, 2002) and concomitantly favor disarticulation, which occurs right after the death (Whatley, 1983) of these microcrustaceans.

Although pyrite formation reflects reducing conditions, its mineralization may be restricted to anoxic sub-environments near the water-sediment interface, under oxidation conditions (Palacios-Fest et al., 1994). These conditions seem to be related to the genesis of pyrite in the ostracod valves in the study area. In interval III, for example, there is a higher incidence of pyritized molds and pyrite-filled carapaces, bioturbation (sample 49) and common presence of oxidation of iron minerals, which indicate oxidizing background conditions (Anadon et al., 1988) and corroborate that the formation of pyrite occurred in anoxic microenvironments (inside the carapaces) under oxidation conditions.

The formation of framboids and euhedral crystals filling the carapaces of ostracods have already been reported by Bennett et al. (2011) and Wang et al. (2013), who inferred early diagenesis conditions and shallow burial depths. However, the occurrence of pyrite does not reflect that the reducing environmental conditions were restricted to micro-environments only; the limiting factor for pyrite mineralization was the low concentration of sulfate in the interstitial waters. This condition

may have prevented the formation of pyrite in larger quantities associated with bioclasts and disseminated in the sediments, as it is a freshwater environment (Marnette et al., 1993). Furthermore, the absence of minerals from marine diagenesis or related to an evaporitic environment further reinforces the freshwater environment hypothesis for the study area.

#### 4.3.3. Late diagenesis mineralization: gypsum formation

Colorless gypsum crystals, with a tabular (Fig. 18B) and acicular habit were identified in two hundred specimens of ostracods in Sample 28, and, albeit occasionally, in Sample 43. The crystals are placed on mono-sulphide and pyrite films, which encrust in some valves and/or carapaces. Gypsum crystals were also observed in iron oxide-altered color valves.

Gypsum can be formed from the weathering of sulphide minerals (Latrubesse et al., 2010) which, when exposed to the oxidation process, has sulfuric acid as one of the by-products of this process. This, in the presence of calcium carbonate and water, forms carbon dioxide and gypsum (Czerewko et al., 2003), as the reaction:

The gypsum formed in the specimens from the study area is of secondary origin and is probably related to the oxidation of pyrite films and mono-sulphide that added sulfuric acid on the carapaces/valves that contained them or in the specimens next to them. Ostracods carapaces and valves served as a nucleation substrate for the formation of this mineral due to its calcite composition.

As confirmed by the XRD results (Table 2), gypsum is absent in the sediments of the analyzed samples, which suggests, in addition to its secondary genesis, low salinity in the deposits in the study area. Gypsum of primary origin precipitates under hypersaline conditions and occurs associated with sediments from evaporitic environments (Nichols, 2009), which discards these paleoenvironmental conditions for the study area.

#### 4.3.4. Dissolution

The dissolution observed in specimens begins in the pore channels and promotes their expansion, regardless of the ontogenetic stage. The partial dissolution term was adopted to characterize only the expansion of the pore-channels (Fig. 18C), while the total dissolution refers to the

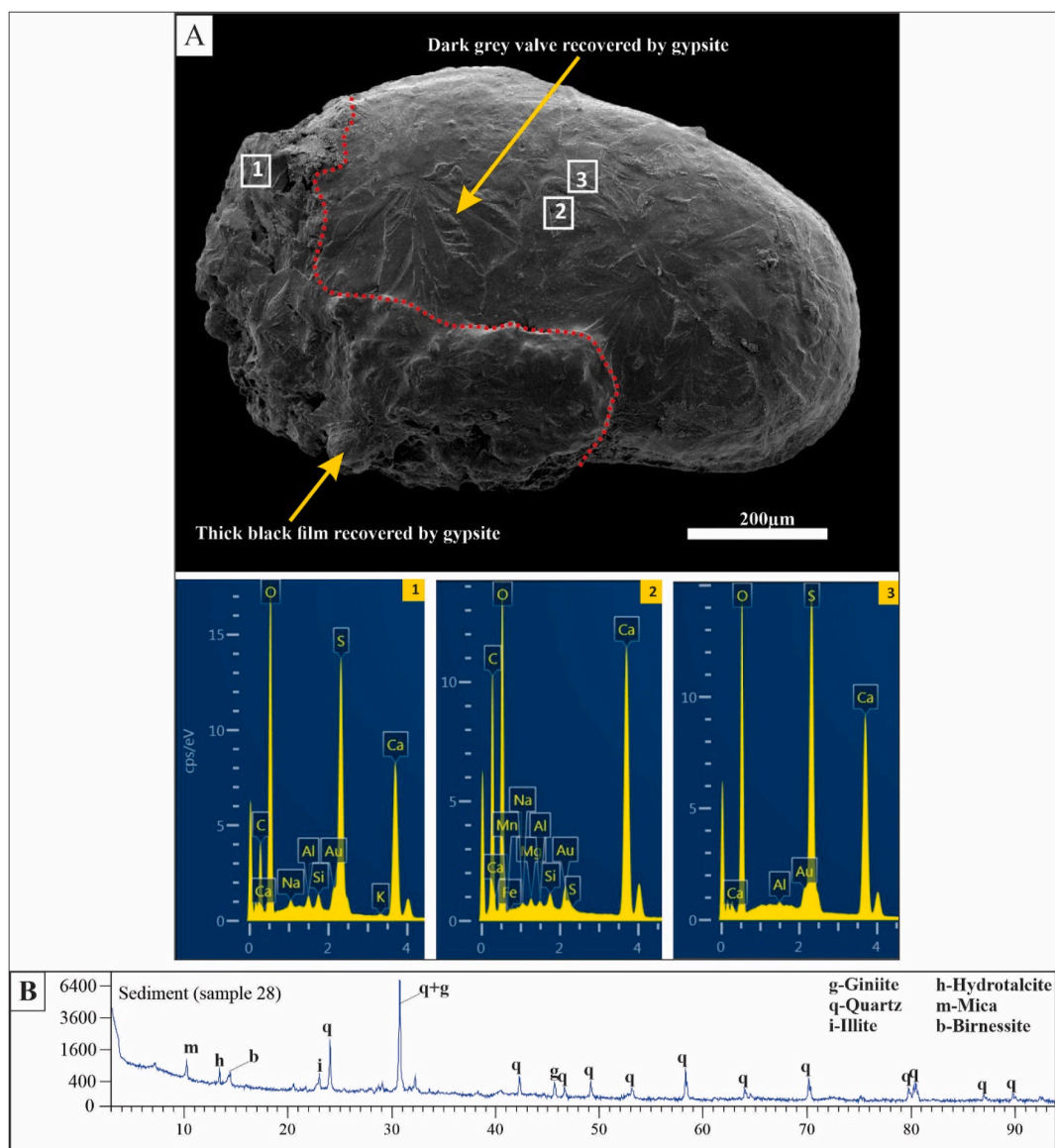


**Fig. 13.** (A) SEM photomicrography and EDS specters (1, 2, 3) in gray valve. Gray valve with part recovered by a thick black film (red dotted) and by gypsum crystals which also recovered the film. (B) Diffractogram with the mineralogical composition of the sediments from where the valve came from. Source: Author.

carapace molds.

Quantitative dissolution analysis shows that it varied significantly between the three intervals (Fig. 16). The results suggest a relationship of this signature with the content of organic matter and oxidation of mono-sulphide.

Interval I was the most affected by dissolution, in which 45% corresponded to molds. In this one, few specimens of ostracods were recovered, which may be a result of the higher organic matter content in samples of locally lignite claystone from this interval. The unsaturation in calcium carbonate due to the acidic pH, both resulting from the high organic matter content, may have promoted the dissolution of smaller juveniles, which justifies the presence of juveniles with sizes close to adults (stages A-3, A -2). Sample 8, for example, has a high concentration of lignite, absence of minerals with a high concentration of iron; no carbonate bioclasts, only 35 pyritized carapace molds. The influence of organic matter content on the dissolution process of ostracods has been frequently reported in lacustrine environments (Mischke et al., 2014, Bergue et al., 2015).

The interval II was where ostracods valves were least affected by dissolution, with a predominance of specimens well preserved,

reflecting the lower content of organic matter, as shown by the lighter gray color of the sediments. However, in the valves/carapaces that have adhering iron mono-sulphide films on their surfaces, it was observed, occasionally (sample 28), some with normal partially expanded pore-channels and some carapaces with whitish portions in the surface (external view). There are also valves with pore-channels filled with mono-sulphide, whose external view is whitish and with adhered gypsum crystals. In these valves, the sulfuric acid released from the oxidation process of the mono-sulphide films may have promoted the partial dissolution of the pore-channels.

The cause of dissolution recorded in the samples from the III interval may be related to bioturbation and oxidation of iron sulphide and mono-sulphide (Brett, 1990). It was found that at depths where bioturbations occur, or close to them, the number of valves with partial dissolution is greater, except in sample 49. This indicates that bioturbations probably favored the exposure and consequent oxidation of the mono-sulphide, and sulphide films adhered to the valves/carapaces (sample 52), resulting in their partial dissolution. Another valid observation is about the influence of giniite films that occur adhered to the valves/carapaces. In sample 49, only 12% of the valves recovered is affected by dissolution

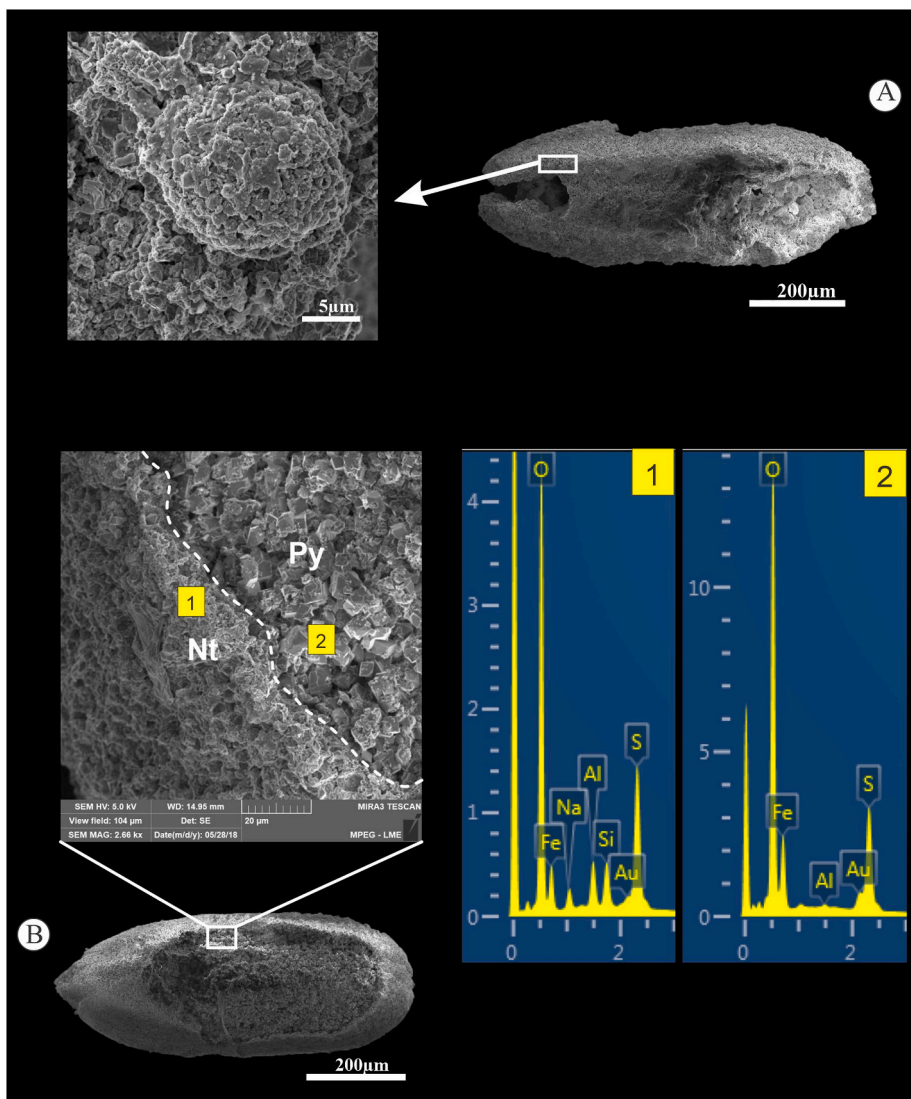


**Fig. 14.** (A–B): SEM photomicrographies. (A) Pyritized ostracod mold. In detail framboidal habit. (B) Pyritized ostracod mold with detail euhedral crystals, natrojarosite crust (Nt) indicated in specter 1 (EDS analysis). The natrojarosite was formed through the pyrite crystals oxidation (Py), indicated in specter 2 (EDS analysis). Source: Author.

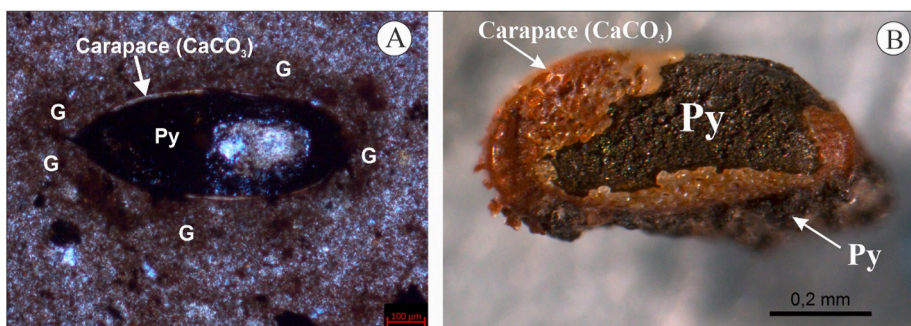


**Fig. 15.** (A) Photomicrography of thin blade (carapace filled by pyrite (Py) and abundance of iron phosphate/giniite (G), reddish-brown color portions, scattered in the sediments matrix that surround the carapace). (B) Pyrite filling the inner part and the surface of ostracod carapace (over-pyrite). Source: Author.

(between partial and total) and 88% of the valves/carapaces covered by a thin film of giniite (iron phosphate), showing no evidence of dissolution (Fig. 17B). The absence of dissolution in specimens covered with iron phosphate may indicate that this mineral was used during the iron reduction process; a process that probably caused alkalinity to be added

to the medium and inhibited the dissolution of the carapaces and valves, despite the environmental conditions unfavorable to preservation, such as bioturbation in sediments and the presence of sulphide. In contrast, in sample 52 (depth 66.12 m) it also presents bioturbation, but the specimens are not covered by giniite. In this sample, 30% of specimens that

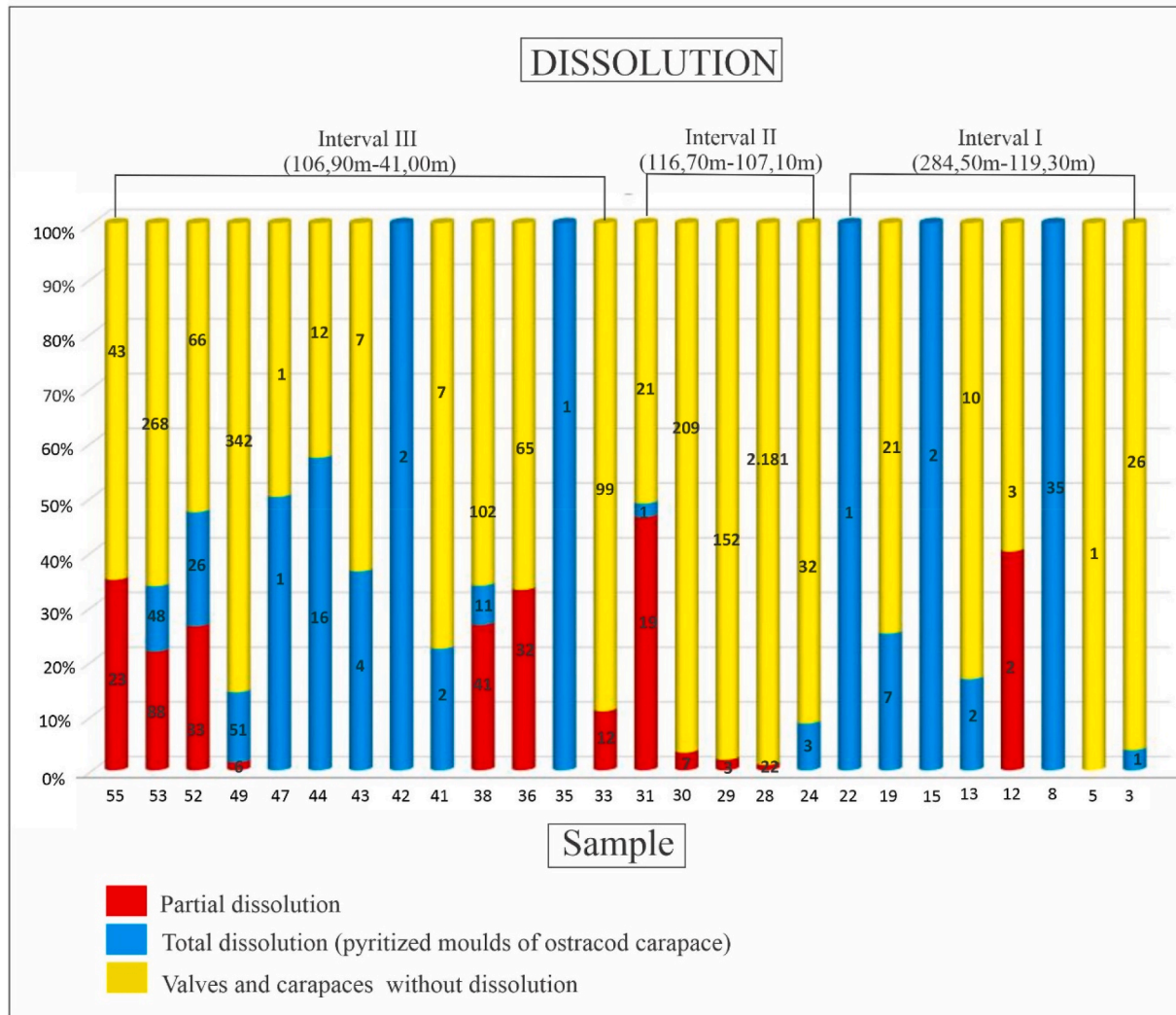


Fig. 16. Percentage histogram showing the valves and carapaces per sample affected or not by dissolution. Source: Author.



Fig. 17. A) Valves/carapaces affected by partial dissolution (red arrows) with iron sulphide and mono-sulphide films adhered to the surface (sample 52). (B) Aspects of the valves and carapaces covered by iron phosphate films (red color specimens), in which the majority were not affected by dissolution (sample 49). Source: Author.

have mono-sulphide and sulphide films on their surface were affected by partial dissolution (Fig. 17A).

#### 4.3.5. Compaction

By examining petrographic thin section, carapaces, and entire ostracod valves without evidence of deformation were observed (Fig. 18A), as well as other bioclasts that do not occur deformed or

reoriented in the matrix. However, fragments of bivalves (Fig. 18D) and larger gastropods are common. These fragments may have been generated, in part, during the process of preparing the thin slides, due to the friable nature of the samples. In general, no evidence of mechanical (fracturing, flattening) and/or chemical compaction (styloclites) was observed in the sediments. Such features suggest shallow burial depths (Boggs Jr, 2006).

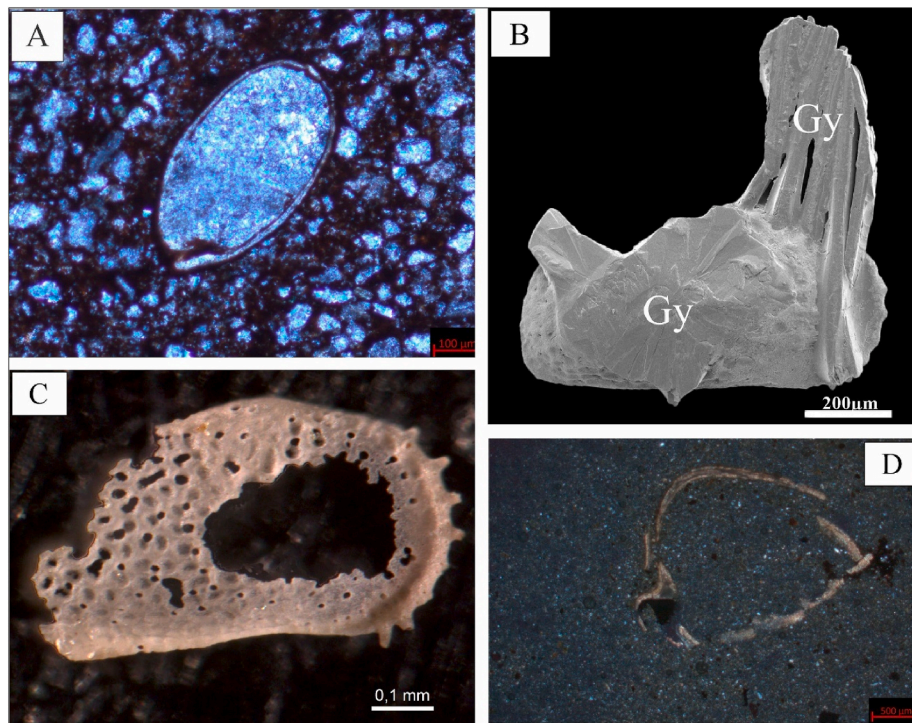


**Fig. 18.** (A, D) Photomicrography of thin section. (B) SEM photomicrography. (C) Imagem from stereomicroscope. (A) Ostracod carapace. (B) Ostracod valve with gypsite crystals (tabular habit) in the carapace surface. (C) Ostracod valve fragmented with poro-channels expanded by dissolution. (D) Fragmented bivalve shell. Source: Author.

#### 4.4. Paleoenvironmental implications

The predominance of fine sedimentation, as seen in the analyzed samples, suggests sediment deposition from suspensions, a characteristic commonly associated with sedimentation in low energy lacustrine environments. The gray color of the sediments, grading to black, shows organic matter and, together with lignite fragments, suggest the contribution of plant material from a nearby marshland environment (Nichols, 2009) (Fig. 19A). For interval I, the absence of bioturbation, the increase in the content of organic matter and poorly preserved fauna, even being absent in some samples, together, suggest reducing and unfavorable conditions for the housing of ostracods, which also justifies the occurrence of allochthonous ostracods in this range. All these features have been recorded in lake bottom deposits (Danielopol et al., 2002; Blome et al., 2014).

The population structure verified in the three intervals shows that the energy of the depositional environment ranged under different energy levels, according to the depth, revealing a control by the wind dynamics over the lake surface and by the influx of terrigenous from the rivers that fed this lake.

In the shallower parts of low-energy lake environments, the action of wind currents on the lake surface can generate weak currents in the substrate (Blome et al., 2014; Mischke et al., 2014), as well as inflows from the rivers that feed the lake, generate resuspension of sediments and in areas close to the discharge, rapid burial events can occur. In this way energy levels can vary in the shallower parts of the lake. As the most likely scenario, it is suggested that the ostracod assemblage from intervals II and III were deposited in the shallower parts of the lake, in the coastal zone, area close to the lake slope (Fig. 19B), as corroborated by the predominance of in situ preservation of the ostracods, indicated by thanatocenosis. Despite the thanatocenoses suggesting some displacement, most of the fauna has a high number of adults and juveniles of various stages, which were not removed from the place where they lived.

Regarding juvenile ostracods that were transported (allochthonous)

and with a good preservation (interval II and III), a short displacement distance is suggested, and within the lake itself. Allochthonous ostracods were probably removed from the coastal area to the lake slope zone, excluding transport from sites outside the lake. For the poorly preserved allochthonous valves from Interval I, it is suggested that it was not the transport itself, but the deposition in sediments rich in organic matter that gave them poor preservation, since valves transported over long distances can remain well preserved (Zhai et al., 2015).

Together, the characteristics mentioned above configure a typical assemblage of a moderate to low energy lake environment in agree with Whatley (1988), Mischke et al. (2014) and Zhai et al. (2015). The good preservation of the valves of the ostracods (mainly of the interval II) may indicate that the low energy conditions, among other parameters, favored the establishment of abundant and well-preserved assemblage in the deposits of the present study, as discussed by Whatley (1988).

Oxidizing conditions are suggested by the occurrence of bioturbations (Anadon et al., 1988), which provided oxidation of iron sulphide/mono-sulphide adhered to the surface of calcite (and aragonitic mollusks) carapaces, as seen in interval III. The oxygenated bottom conditions are also suggested by the establishment of abundant fauna of gastropods, bivalves, ostracods, in addition to the presence of charophytes and fish remains (range II and III), similarly observed in the coastal zone of a perennial lake by Blomeier et al. (2003) (Fig. 19B).

The occurrence of pyrite associated with ostracods (and other bioclasts) cannot by itself indicate reducing conditions, since the genesis of pyrite in the present work took place in the microenvironment of the carapaces, under oxidizing environmental conditions, as observed in interval III.

The low salinity of the depositional environment is, in turn, evidenced by the absence of evaporitic minerals (gypsum, sylvite, anhydrite; Nichols, 2009; Boggs Jr, 2006). The absence of pyrite in the sediments, despite the availability of detrital iron and organic matter (Wang et al., 2013), indicates that freshwater conditions constituted the limiting factor for the formation of this mineral in the sediments of the study area.

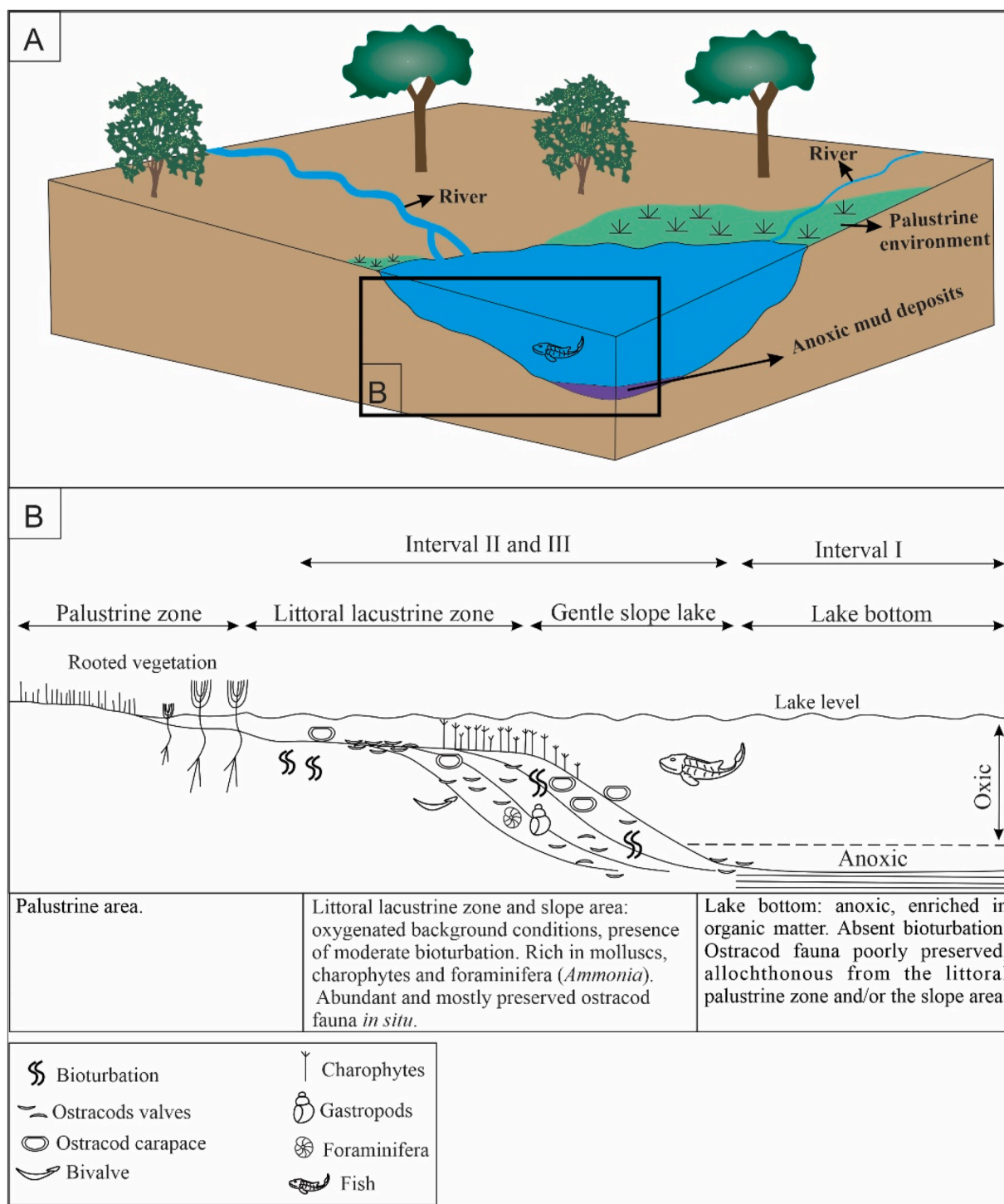


Fig. 19. (A) Bloccodiagram with the paleoenvironmental reconstitution of the studied core 1AS-5-AM. (B) Intervals recognized in the studied core and the respective sub-environments of the lake. Source: modified by Blomeier et al. (2003).

It is worth mentioning that despite the occurrence of an indicative rate of brackish/marine water, such as *Skopaeocythere tetrakanthos*, *Perissocytheridea*, and *Pellucistoma* (Gross et al., 2015), in addition to the significant number of foraminifera of the genus *Ammonia* in sample 28, the results obtained here corroborate freshwater conditions. The low quantity and the occurrence only of very delicate juvenile valves of these species may indicate that the weak development and fragility of the carapaces is due to the environmental stress caused by the freshwater conditions.

From the X-ray diffraction analysis, it was verified that the

mineralogical assemblage, as well as the organic matter content exerted a significant influence on the preservation status of the ostracod's assemblage.

The occurrence of specific minerals such as iron phosphate shows that the understanding of the composition of sediments must be considered, since fossil-diagenesis processes can be dependent on the mineralogy of the sediments, as seen in the present study. As the distinction of mineralogical assemblage, it was also important to distinguish the presence of minerals that do not reflect the natural conditions of the depositional environment, as seen by the occurrence of

Intervals	Sample (Depth)	Adults vs. juveniles (Brouwers,1988)					Types of associations (Boomer et al., 2003)
		Valve	Carapace	Adults (A)	Juveniles (J)	Ratio A/J	
Interval III	55 (41.00 m)	16A, 9J	6A, 11J	22	20	1/1	High energy thanatocoenoses
	53 (65.92 m)	118A, 38J	99A, 13J	217	51	4/1	
	52 (66.12 m)	30A, 19J	10A, 8J	40	27	1.4/1	
	49 (73.60 m)	7A, 173J	5A, 157J	12	330	1/27.5	Interrupted thanatocoenoses
	44 (78.80 m)	4A, 7J	1J	4	8	1/2	Low energy taphocoenosis
	43 (81.12 m)	6A, 1J		6	1	6/1	High energy thanatocoenoses
	38 (97.65 m)	27A, 47J	15A, 13J	42	60	1/1.4	Low energy taphocoenosis
	36 (99.30 m)	6A, 34J	25J	6	59	1/9.8	
	33 (105.45 m)	2A, 37J	9A, 51J	11	88	1/8	Interrupted thanatocoenoses
Interval II	31 (107.10 m)	10A, 7J	1A, 3J	11	10	1/1	High energy thanatocoenoses
	30 (107.55 m)	15A, 188J	6J	15	194	1/12.9	Low energy taphocoenosis
	29 (109.55 m)	42A, 34J	61A, 15J	103	49	2/1	Low energy thanatocoenoses
	28 (110.20 m)	1,170A, 544J	394A, 73J	1,564	617	2.5/1	
	24 (114.20 m)	10J	1A, 21J	1	31	1/31	Interrupted thanatocoenoses
Interval I	19 (127.00 m)	1A, 18J	1A, 1J	2	19	1/9.5	Low energy taphocoenosis
	13 (142.70 m)	1A, 7J	1A, 1J	2	8	1/4	
	3 (237.00 m)	21A, 4J	1A	22	4	5.5/1	High energy thanatocoenoses

Chart 1. Analysis of the population structure in the three intervals of core 1AS-5-AM. Source: Author.

natrojarosite, which indicated oxidizing conditions in a location evidenced as a reducer.

## 5. Conclusions

The taphonomic analysis on Miocene ostracods assemblage from Solimões Formation, recovered from the core 1AS-5-AM, allowed us to verify that, in general, there was no substitution during the fossilization process, although the following elements were observed: 1) valves and ostracod carapaces covered with films of mono-sulphide, iron phosphate, and iron and thallium sulphide; 2) preserved in iron oxides, 3) recrystallized; as 4) pyritized carapace molds; and 5) white hyaline valves. Right after burial, siliciclastic sediments were the main contaminating source for the carapaces. After the mineralization of sulphide and mono-sulphide (inside and on the surface of the valves/carapaces) and their subsequent oxidation, the iron oxides and sulfate minerals resulting from this process also became part of the group of minerals carrying contaminating elements in the carapaces. The carapaces/valves analyzed, despite the contaminating elements, remained with the original chemical composition preserved, a fact that reflects the

mineral stability of the low magnesian calcite of the valves and the little post-mortem transport provided by the stability of a calm environment, as well as shallow burial depth.

Biostratinomic alterations correspond to fragmentation, transport, disarticulation, and bioerosion. Fragmentation was not indicated to be safe as an indication of the natural conditions of the paleoenvironment, as a good part of it may have been generated during the laboratory stage. On the other hand, fossil-diagenetic alterations include mineral filling by pyrite, dissolution, recrystallization, and color change, which only reflect conditions of early and late diagenesis, in addition to superficial burial. As an environment, it is suggested a lacustrine of moderate to low energy and low salinity, corroborating with the paleoenvironmental interpretations of the Miocene deposits of the Solimões Formation.

For the taphonomic characterization, specifically of ostracods, additional techniques such as x-ray diffraction (XRD), scanning electron microscopy (SEM) combined with energy dispersive spectrometry (EDS), in addition to the traditional petrographic thin section analysis were indispensable for accuracy of taphonomic analysis – a fundamental criterion in the reconstruction of a paleoenvironment.

This study is the first well-documented case about the diagenetic

history of the ostracods from the Solimões Formation.

### CRedit authorship contribution statement

**Katiane Silva dos Santos:** Writing – review & editing, Writing – original draft, Resources, Methodology, Investigation, Data curation, Conceptualization. **Maria Inês Feijó Ramos:** Writing – review & editing, Validation, Supervision, Project administration, Investigation, Funding acquisition.

### Declaration of competing interest

The authors declare that they have no known competing financial interests or personal relationships that could have appeared to influence the work reported in this paper.

### Data availability

Data will be made available on request.

### Acknowledgments

The authors would like to thank the Museu Paraense Emílio Goeldi (MPEG) for the infrastructure provided by the laboratories of the Coordenação de Ciências da Terra e Ecologia. The Federal University of Pará (UFPA) supported this research through the Graduate Program in Geology and Geochemistry (PPGG). The authors thank the Editor and anonymous reviewers for improving the article. This work was carried out with the support of the Coordenação de Aperfeiçoamento de Pessoal de Nível Superior - Brazil (CAPES – financing code 001) and the Brazilian Council of Science and Technological Development (productivity fellowships grant 307424/2019–7 to M.I.F.R.).

### References

- Allison, P.A., 1990. Taphonomy: decay process. In: Briggs, D.E.G., Crowther, P.R. (Eds.), *Paleobiology: a Synthesis*. Blackwell Scientific, Oxford, pp. 213–216.
- Anadón, P., Cabrera, L., Julià, R., 1988. Anoxic-oxic cyclical lacustrine sedimentation in the Miocene Rubielos de Mora Basin, Spain. *Geological Society, London, Special Publications* 40 (1), 353–367. <https://doi.org/10.1144/GSL.SP.1988.040.01.29>.
- Bennett, C.E., Williams, M., Leng, M.J., Siveter, D.J., Davies, S.J., Sloane, H.J., Wilkinson, I.P., 2011. Diagenesis of fossil ostracods: implications for stable isotope based palaeoenvironmental reconstruction. *Palaeogeogr. Palaeoclimatol. Palaeoecol.* 305, 150–161. <https://doi.org/10.1016/j.palaeo.2011.02.028>.
- Bergue, C.T., Maranhão, M.D.S.A., Fauth, G., 2015. Paleolimnological inferences based on Oligocene ostracods (Crustacea: ostracoda) from Tremembé Formation, southeast Brazil. *An Acad. Bras Ciências* 87 (3), 1531–1544. <https://doi.org/10.1590/0001-3765201520140366>.
- Bertanni, R.T., Carozzi, A.V., 1985. Lagoa Feia Formation (lower Cretaceous), Campos basin, offshore Brazil: rift valley stage lacustrine carbonate reservoirs. *J. Petrol. Geol.* 8 (1), 37–58. <https://doi.org/10.1111/j.1747-5457.1985.tb00190.x>.
- Blome, M.W., Cohen, A.S., Lopez, M.J., 2014. Modern distribution of ostracods and other limnological indicators in southern lake Malawi: implications for paleocological studies. *Hydrobiologia* 728 (1), 179–200. <https://doi.org/10.1007/s10750-014-1817-5>.
- Blomeier, D., Wisshak, M., Joachimski, M., Freiwald, A., Volohonsky, E., 2003. Calcareous, alluvial and lacustrine deposits in the old red sandstone of central north spitsbergen (wood bay formation, early devonian). *Norwegian Journal of Geology/ Norsk Geologisk Forening* 83 (4), 281–298.
- Diagenesis of siliciclastic sedimentary rocks. In: Boggs Jr., S. (Ed.), 2006. *Principles of Sedimentology and Stratigraphy*. Pearson Education, Upper Saddle River, New Jersey, pp. 145–151.
- Boomer, I., Horne, D.J., Slipper, I.J., 2003. The use of ostracods in palaeoenvironmental studies, or what can you do with an ostracod shell? In: Park, L.E., Smith, A.J. (Eds.), *Bridging The Gap: Trends in the Ostracode Biological and Geological Sciences*. The Paleontological Society Papers, New Haven, pp. 153–180. <https://doi.org/10.1017/S1089332600002199>.
- Brett, C.E., 1990. Destructive taphonomic processes and skeletal durability. In: Briggs, D. E.G., Crowther, P.R. (Eds.), *Paleobiology: a Synthesis*. Blackwell Scientific, Oxford, pp. 223–226.
- Brouwers, E.M., 1988. Sediment transport detected from the analysis of ostracod population structure: an example from the Alaskan continental shelf. In: De Deckker, P., Colin, J.-P., Peyrouquet, J.-P. (Eds.), *Ostracoda in the Earth Sciences*. Elsevier, Amsterdam, pp. 231–244.
- Caputo, M.V., 1984. *Stratigraphy, Tectonics, Paleoclimatology and Paleogeography of Northern Basins of Brazil*. PhD Thesis. Universidade da California, Santa Barbara, USA, p. 603p.
- Cruz, N.M.C., 1984. Palinologia do linhito do Solimões, estado do Amazonas. In: 2° Symposium Amazônico, Manaus, Anais, pp. 473–480.
- Czerewko, M.A., Cripps, J.C., Duffell, C.G., Reid, J.M., 2003. The distribution and evaluation of sulfur species in geological materials and manmade fills. *Cement Concr. Compos.* 25 (8), 1025–1034. [https://doi.org/10.1016/S0958-9465\(03\)00126-4](https://doi.org/10.1016/S0958-9465(03)00126-4).
- Danielopol, D.L., Casale, L.M., Olteanu, R., 1986. On the preservation of carapaces of some limnic ostracods: an exercise in actuopalaeontology. *Hydrobiologia* 143, 143–157. <https://doi.org/10.1007/BF00026657>.
- Danielopol, D.L., Ito, E., Wansard, G., Kamiya, T., Cronin, T.M., Baltanas, A., 2002. Techniques for collection and study of Ostracoda. In: Holmes, J.A., Chivas, A.R. (Eds.), *The Ostracoda: Applications in Quaternary Research*. Washington: D.C., vol. 131 American Geophysical Union, pp. 65–97. <https://doi.org/10.1029/131GM04> (Geophysical Monograph 131).
- DeDeckker, P., 2002. Ostracod paleoecology. In: Holmes, J.A., Chivas, A.R. (Eds.), *The Ostracoda: Applications in Quaternary Research*, Geophysical Monograph 131. D.C., American Geophysical Union, Washington, pp. 99–120.
- DeDeckker, P., 2017. Trace elemental distribution in ostracod valves. From solution ICPMS and laser ablation ICPMS to microprobe mappicoimbrng: a tribute to Rick Forester. *Hydrobiologia* 786, 23–39.
- Do Carmo, D.A., Whatley, R.C., Timberlake, S., 1999. Variable nodding and palaeoecology of a Middle Jurassic limnocytherid ostracod: implications for modern brackish water taxa. *Palaeogeogr. Palaeoclimatol. Palaeoecol.* 148 (1–3), 23–35.
- Eiras, J.F., Becker, C.R., Souza, E.M., Gonzaga, J.G., Da Silva, J.G.F., Daniel, L.M.F., Matsuda, N.S., Feijó, F.J., 1994. Bacia do Solimões. *Boletim de Geociências da Petrobras, Rio de Janeiro* 8 (1), 17–46.
- Gross, M., Piller, W.E., Ramos, M.I., Silva Paz, J. D. da, 2011. Late Miocene sedimentary environments in south-western Amazonia (Solimões formation; Brazil). *J. S. Am. Earth Sci.* 32 (2), 169–181. <https://doi.org/10.1016/j.jsames.2011.05.004>.
- Gross, M., Ramos, M.I.F., Caporaletti, M., Piller, W.E., 2013. Ostracods (Crustacea) and their palaeoenvironmental implication for the Solimões Formation (late Miocene; western amazonia/Brazil). *J. S. Am. Earth Sci.* 42, 216–241. <https://doi.org/10.1016/j.jsames.2012.10.002>.
- Gross, M., Ramos, M.I.F., Piller, W.E., 2014. On the Miocene Cyprideis species flock (ostracoda; Crustacea) of western amazonia (Solimões Formation): refining taxonomy on species level. *Zootaxa* 3899 (1), 1–69. <https://doi.org/10.11646/zootaxa.3899.1.1>.
- Gross, M., Ramos, M.I.F., Werner, E.P., 2015. A minute ostracod (Crustacea: cytheromatidae) from the Miocene Solimões Formation (western Amazonia, Brazil): evidence for marine incursions? *J. Syst. Palaeontol.* 14 (7), 581–602. <https://doi.org/10.1080/14772019.2015.1078850>.
- Holmes, J.A., 1992. Nonmarine ostracods as Quaternary palaeoenvironmental indicators. *Prog. Phys. Geogr.* 16 (4), 405–431. <https://doi.org/10.1177/030913339201600402>.
- Holmes, J.A., 1997. The palaeoenvironmental significance of iron and manganese in non-marine ostracod shells: a preliminary analysis. In: Holmes, J.A., Lynch, K. (Eds.), *The Kingston Papers: a Geographical Perspective on the Environment, Economy and Society*. Kingston University, Kingston upon Thames, pp. 198–212.
- Holmes, J.A., De Deckker, P., 2012. The chemical composition of ostracod shells: applications in Quaternary palaeoclimatology. In: Horne, D.J., Holmes, J.A., Rodriguez-Lazaro, J., Viehberg, F.A. (Eds.), *Developments in Quaternary Sciences*. Elsevier, Oxford, UK, pp. 131–143. <https://doi.org/10.1016/B978-0-444-53636-5.00008-1>.
- Hoorn, C., 1993. Marine incursions and the influence of Andean tectonics on the Miocene depositional history of northwestern Amazonia: results of a palynostratigraphic study. *Palaeogeogr. Palaeoclimatol. Palaeoecol.* 105, 267–309. [https://doi.org/10.1016/0031-0182\(93\)90087-Y](https://doi.org/10.1016/0031-0182(93)90087-Y).
- Hoorn, M.C., 1994. Fluvial palaeoenvironments in the intracratonic Amazon basin (early miocene-early middle Miocene, Colombia). *Palaeogeogr. Palaeoclimatol. Palaeoecol.* 109, 1–54. [https://doi.org/10.1016/0031-0182\(94\)90117-1](https://doi.org/10.1016/0031-0182(94)90117-1).
- Hoorn, C., Wesselingh, F.P., Hovikoski, J., Guerrero, J., 2010. The development of the amazonian mega-wetland (Miocene; Brazil, Colombia, Peru, bolívia). In: Hoorn, C., Wesselingh, F. (Eds.), *Amazonia: Landscape and Species Evolution, a Look into the Past*. Wiley-Blackwell publications, Oxford, UK. <https://doi.org/10.1002/9781444306408.ch8>.
- Jaramillo, C., Romero, I., D'Apolito, C., Bayona, G., Duarte, E., Louwey, S., Escobar, J., Luque, J., Carrillo-Briceno, J.D., Zapata, V., Mora, A., Schouten, S., Zavada, M., Harrington, G., Ortiz, J., Frank, P., Wesselingh, F.P., 2017. Miocene flooding events of western Amazonia. *Sci. Adv.* <https://doi.org/10.1126/sciadv.1601693>.
- Keyser, D., Walter, R., 2004. Calcification in ostracodes. *Rev. Espanola Micropaleontol.* 36, 1–11.
- Kihn, R.G., Crespo, F., Pall, J.L., 2017. Ostracódeos de lagos someros de la región Central de Argentina: implicaciones paleolimnológicas. *Rev. Bras. Palaontol.* 20 (3), 373–382. <https://doi.org/10.4072/rbp.2017.3.08>.
- Latrubesse, E.M., Cozzuol, M., Silva-Caminha, S.A.F., Rigby, C.A., Apsy, M.L., Jaramillo, C.A., 2010. The late Miocene paleogeography of the Amazon basin and the evolution of the Amazon River system. *Earth Sci. Rev.* 99, 99–124. <https://doi.org/10.1016/j.earscirev.2010.02.005>.
- Leandro, L.M., Linhares, A.P., Lira Mota, M.A.D., Fauth, G., Santos, A., Villegas-Martin, J., Vieira, C.E.L., Bruno, M.D.R., Lee, B., Baecker-Fauth, S., Lopes, F.M., Ramos, M.I.F., 2022. Multi-proxy evidence of caribbean-sourced marine incursions in the Neogene of western amazonia, Brazil. *Geology* 50 (4), 465–469. <https://doi.org/10.1130/G49544.1>.

- Linhares, A.P., Ramos, M.I.F., Gaia, V.C.S., 2017. The significance of marine microfossils for paleoenvironmental reconstruction of the Solimões Formation (Miocene), western Amazonia, Brazil. *J. S. Am. Earth Sci.* 79, 57–66. <https://doi.org/10.1016/j.jsames.2017.07.007>.
- Linhares, A.P., Ramos, M.I., Gaia, V.C., Friaes, Y.S., 2019. Integrated biozonation based on palynology and ostracods from the Neogene of Solimões Basin, Brazil. *J. S. Am. Earth Sci.* 91, 57–70. <https://doi.org/10.1016/j.jsames.2019.01.015>.
- Linhares, A.P., Ramos, M.I.R., Gross, M., Piller, W.E., 2011. Evidence for marine influx during the Miocene in southwestern Amazonia, Brazil. *Geol. Colomb.* 36 (1), 91–104.
- Machado, L.G., Scheel-Ybert, R., Robson, T.B., Araujo, C. M. de, 2012. Lenhos fósseis do Neógeno da Bacia do Acre, Formação Solimões: contexto paleoambiental. *Rev. Bras. Geociências* 42 (1), 67–80. <https://doi.org/10.25249/0375-7536.20124216780>.
- Maia, R.G.N., Godoy, H.K., Yamaguti, H.S., Moura, P.A., Costa, F.S.F., Holanda, M.A., Costa, J.A., 1977. Projeto Carvão No Alto Solimões. Relatório Final. Companhia de Pesquisa de Recursos Minerais-Departamento Nacional da Produção Mineral, Manaus, p. 142.
- Marnette, E.C., Van Breemen, N., Hordijk, K.A., Cappenberg, T.E., 1993. Pyrite formation in two freshwater systems in The Netherlands. *Geochim. Cosmochim. Acta* 57 (17), 4165–4177. [https://doi.org/10.1016/0016-7037\(93\)90313-L](https://doi.org/10.1016/0016-7037(93)90313-L).
- Matzke-Karasz, R., Neil, J.V., Smith, R.J., Godthelp, H., Archer, M., Hand, S.J., 2013. Ostracods (Crustacea) with soft part preservation from Miocene cave deposits of the riversleigh world heritage area, NW queensland, Australia. *J. Syst. Palaeontol.* 11 (7), 789–819. <https://doi.org/10.1080/14772019.2012.760007>.
- Mischke, S., Ashkenazi, S., Almogi-Labin, A., Goren-Inbar, N., 2014. Ostracod evidence for the acheulian environment of the ancient hula lake (levant) during the early-mid pleistocene transition. *Palaeogeography, Palaeoclimatology, Palaeoecol. Jaramillo ogy* 412, 148–159. <https://doi.org/10.1016/j.palaeo.2014.07.036>.
- Munoz-Torres, F.A., Whatley, R.C., Van Harten, D., 2006. Miocene ostracod (Crustacea) biostratigraphy of the upper Amazon basin and the Cyprideis genus evolution. *J. S. Am. Earth Sci.* 21, 75–86. <https://doi.org/10.1016/j.jsames.2005.08.005>.
- Namioiko, T., Danielopol, D.L., Grafenstein, U., von Lauterbach, S., Brauer, A., Andersen, N., Huls, M., Milecka, K., Baltana's, A., Geiger, W., Declakes, P., 2015. Palaeoecology of Late Glacial and Holocene profundal Ostracoda of pre-Alpine lake Mondsee (Austria) – a base for further (palaeo)biological research. *Palaeogeogr. Palaeoclimatol. Palaeoecol.* 419, 23–36. <https://doi.org/10.1016/j.palaeo.2014.09.009>.
- Nichols, G. (Ed.), 2009. *Sedimentology and Stratigraphy*. John Wiley & Sons, UK.
- Nogueira, A.C.R., Arai, M., Horbe, A.M.C., Horbe, M.A., Silveira, R.R., Silva, J.S., Motta, M.B., 2003. The marine influence on the Solimões Formation deposits in the Coari region (AM): record of the Miocene transgression in the Western Amazon. *SBG, 8th Amazon Geology Symposium, Manaus, Amazonas 1*, 468–472.
- Nogueira, A.C.R., Silveira, R.R., Guimarães, J.T.F., 2013. Neogene-Quaternary sedimentary and paleovegetation history of eastern Solimões Basin, central Amazon region. *Journal of South American Earth Sciences* 46, 89–99. <https://doi.org/10.1016/j.jsames.2013.05.004>.
- Palacios-Fest, M.R., Cohen, A.S., Anadón, P., 1994. Use of ostracodes as paleoenvironmental tools in the interpretation of ancient lacustrine records. *Rev. Esp. Palaontol.* 9 (2), 145–164.
- Park, L.E., Cohen, A.S., Martens, K., Bralek, R., 2003. The impact of taphonomic processes on interpreting paleoecologic changes in large lake ecosystems: ostracodes in Lakes Tanganyika and Malawi. *J. Paleolimnol.* 30 (2), 127–138. <https://doi.org/10.1023/A:1025570032179>.
- Purper, I., Ornellas, L., 1991. New ostracodes of endemic fauna of the Pebas formation, upper. *Pesquisas* 18 (1), 25–30. <https://doi.org/10.22456/1807-9806.21359>.
- Purper, I., Pinto, I.D., 1983. New genera and species of ostracodes of the upper Amazon basin, Brasil. *Pesquisas* 15, 113–126. <https://doi.org/10.22456/1807-9806.21726>.
- Raiswell, R., 1997. A geochemical framework for the application of stable sulphur isotopes to fossil pyritization. *J. Geol. Soc.* 154, 343–356. <https://doi.org/10.1144/gsjgs.154.2.0343>.
- Ramos, M.I.F., 2006. Ostracods from the Neogene Solimões Formation (Amazonas, Brazil). *J. S. Am. Earth Sci.* 21, 87–95. <https://doi.org/10.1016/j.jsames.2005.08.001>.
- Räsänen, M.E., Linna, A.M., Santos, J.C., Negri, F.R., 1995. Late Miocene tidal deposits in the Amazonian foreland basin. *Science* 269, 386–390. <https://doi.org/10.1126/science.269.5222.386>.
- Silveira, R.R., Souza, P.A., 2017. Palinoestratigrafia da Formação Solimões na região do alto Solimões (Atalaia do Norte e Tabatinga), Amazonas, Brasil. *Geociências, UNESP* 36 (1), 100–117.
- Siveter, D.J., Tanaka, G., Farrell, Ú.C., Martin, M.J., Siveter, D.J., Briggs, D.E.G., 2014. Exceptionally preserved 450-million-year-old ordivician ostracods with brood care. *Curr. Biol.* 24 (7), 801–806.
- Smith, A.J., Horne, D.J., 2002. Ecology of marine, marginal marine and nonmarine ostracodes. In: Holmes, J.A., Chivas, A.R. (Eds.), *The Ostracoda: Applications in Quaternary Research*, Geophysical Monograph 131. D.C., American Geophysical Union, Washington, pp. 37–64. <https://doi.org/10.1029/131GM03>.
- Tucker, M.E., 1990. Diagenesis: skeletal carbonates. In: Briggs, D.E.G., Crowther, P.R. (Eds.), *Palaeobiology: a Synthesis*. Blackwell Scientific Publications, London, pp. 247–250. <https://doi.org/10.1306/74D717D5-2B21-11D7-8648000102C1865D>.
- Turpen, J.B., Angell, R.W., 1971. Aspects of molting and calcification in the ostracod *Heterocypris*. *Biol. Bull.* 140 (2), 331–338. <https://doi.org/10.2307/1540077>.
- Urbani, F., Grande, S., Mendi, D., Gómez, A., Reategui, W., Melo, L., Carreño, R., 2016. *Espeleología, V. Minerales Secundarios de la Región Septentrional de los Estados Lara y Yaracuy*, vol. 32. Academia Nacional de la Ingeniería y el Hábitat, pp. 137–163.
- Wanderley Filho, J.R., Eiras, J.F., Cunha, P.R.C., van der Ven, P.H., 2010. The paleozoic Solimões and Amazonas basins and the Acre foreland basin of Brazil. In: Hoorn, C., Wesselingh, F.P. (Eds.), *Amazonia, Landscape and Species Evolution: A Look into the Past*. Wiley-Blackwell, Oxford, pp. 29–37. <https://doi.org/10.1002/9781444306408.ch3>.
- Wang, P., Huang, Y., Wang, C., Feng, Z., Huang, Q., 2013. Pyrite morphology in the first member of the late cretaceous qingshankou formation, songliao basin, northeast China. *Palaeogeogr. Palaeoclimatol. Palaeoecol.* 385, 125–136. <https://doi.org/10.1016/j.palaeo.2012.09.027>.
- Wesselingh, F.P., Hoorn, M.C., Guerrero, J., Räsänen, M.E., Romero, P.L., Salo, J., 2002. The stratigraphy and regional structure of Miocene deposits in western Amazonia (Peru, Colombia and Brazil), with implications for Late Neogene landscape evolution. *Scripta Geol.* 133, 291–322.
- Wesselingh, F.P., Ramos, M.I.F., 2010. Amazonian aquatic invertebrate faunas (Mollusca, ostracoda) and their development over the past 30 million years. In: *Amazonia: Landscape and Species Evolution*. Wiley-Blackwell Publishing Ltd., Oxford, UK, pp. 302–316.
- Whatley, R.C., 1983. The application of Ostracoda to paleoenvironmental analysis. In: Maddorocks, R.F. (Ed.), *Applications of Ostracoda*. University of Houston Press, Houston, pp. 51–77.
- Whatley, R.C., 1988. Population structure of ostracods: some general principles for the recognition of palaeoenvironments. In: De Deckker, P., Colin, J.P. y Peypouquet J.P. (Eds.), *Ostracoda in the Earth Sciences*. Elsevier, Amsterdam, pp. 245–256.
- Whatley, R.C., Muñoz-Torres, F., van Harten, D., 1998. The ostracoda of an isolated Neogene saline lake in the western Amazon basin. *Bulletin Centre Recherches Elf Exploration Production Mémoires* 20, 231–245.
- Wilkinson, I.P., Wilby, P.R., Williams, M., Siveter, D.J., Page, A.A., Leggitt, L., Riley, D. A., 2010. Exceptionally preserved ostracodes from a Middle Miocene palaeolake, California, USA. *J. Geol. Soc.* 167 (4), 817–825. <https://doi.org/10.1144/0016-76492009-178>.
- Williams, M., Siveter, D.J., Ashworth, A.C., Wilby, P.R., Horne, D.J., Lewis, A.R., Marchant, D.R., 2008. Exceptionally preserved lacustrine ostracods from the Middle Miocene of Antarctica: implications for high-latitude palaeoenvironment at 77 south. *Proc. Biol. Sci.* 275, 2449–2454. <https://doi.org/10.1098/rspb.2008.0396>.
- Zhai, D., Xiao, J., Fan, J., Wen, R., Pang, Q., 2015. Differential transport and preservation of the instars of *Limnocythere inopinata* (Crustacea, Ostracoda) in three large brackish lakes in northern China. *Hydrobiologia* 747 (1), 1–18. <https://doi.org/10.1007/s10750-014-2118-8>.